# NAVAL POSTGRADUATE SCHOOL
## Monterey, California


# THESIS

**NONLINEAR OSCILLATIONS OF A TRIATOMIC MOLECULE**

by

Sean Odell Wilson

June 2002

| | |
|---|---|
| Thesis Advisor: | Bruce Denardo |
| Second Reader: | Andres Larraza |

THIS PAGE INTENTIONALLY LEFT BLANK

| REPORT DOCUMENTATION PAGE | | | Form Approved OMB No. 0704-0188 |
|---|---|---|---|
| Public reporting burden for this collection of information is estimated to average 1 hour per response, including the time for reviewing instruction, searching existing data sources, gathering and maintaining the data needed, and completing and reviewing the collection of information. Send comments regarding this burden estimate or any other aspect of this collection of information, including suggestions for reducing this burden, to Washington headquarters Services, Directorate for Information Operations and Reports, 1215 Jefferson Davis Highway, Suite 1204, Arlington, VA 22202-4302, and to the Office of Management and Budget, Paperwork Reduction Project (0704-0188) Washington DC 20503. | | | |
| **1. AGENCY USE ONLY** ***(Leave blank)*** | **2. REPORT DATE** June 2002 | **3. REPORT TYPE AND DATES COVERED** Master's Thesis | |
| **4. TITLE AND SUBTITLE**: Title (Mix case letters) NONLINEAR OSCILLATIONS OF A TRIATOMIC MOLECULE | | | **5. FUNDING NUMBERS** |
| **6. AUTHOR(S) Wilson, Sean O.** | | | |
| **7. PERFORMING ORGANIZATION NAME(S) AND ADDRESS(ES)** Naval Postgraduate School Monterey, CA 93943-5000 | | | **8. PERFORMING ORGANIZATION REPORT NUMBER** |
| **9. SPONSORING /MONITORING AGENCY NAME(S) AND ADDRESS(ES)** N/A | | | **10. SPONSORING/MONITORING AGENCY REPORT NUMBER** |
| **11. SUPPLEMENTARY NOTES** The views expressed in this thesis are those of the author and do not reflect the official policy or position of the Department of Defense or the U.S. Government. | | | |
| **12a. DISTRIBUTION / AVAILABILITY STATEMENT** Approved for public release; distribution is unlimited | | | **12b. DISTRIBUTION CODE** |

**13. ABSTRACT** ***(maximum 200 words)***

Due to nonlinearity in the coupling, one of the vibrational modes of a straight symmetric triatomic molecule can be unstable for amplitudes greater than a threshold value. The instability is due to the mode parametrically exciting another mode. The threshold amplitude decreases if the difference of the frequency of the two modes is reduced. We consider the simplest case of a symmetric rectilinear molecule where the coupling has a cubic nonlinearity in addition to a linear restoring force. Approximate analytical results are in good agreement with numerical simulations of the exact equations of motion, although in some cases the actual behavior fundamentally deviates from the perturbative theory. Two physical demonstrations of the instability are described, where the apparatus are a system of gliders coupled by springs and magnets on an air track. Possible quantum mechanical implications are discussed. This work is a fundamental generalization of the parametric instability of two linearly coupled nonlinear oscillators that was reported in a previous investigation.

| **14. SUBJECT TERMS** Parametric Excitation, Nonlinear Oscillations, Symmetric Rectilinear Triatomic Molecule, Nonlinear Coupling, Triatomic Molecule. | | | **15. NUMBER OF PAGES** 73 |
|---|---|---|---|
| | | | **16. PRICE CODE** |
| **17. SECURITY CLASSIFICATION OF REPORT** Unclassified | **18. SECURITY CLASSIFICATION OF THIS PAGE** Unclassified | **19. SECURITY CLASSIFICATION OF ABSTRACT** Unclassified | **20. LIMITATION OF ABSTRACT** UL |

NSN 7540-01-280-5500 Standard Form 298 (Rev. 2-89)
Prescribed by ANSI Std. 239-18

THIS PAGE INTENTIONALLY LEFT BLANK

**Approved for public release; distribution is unlimited**

**NONLINEAR OSCILLATIONS OF A TRIATOMIC MOLECULE**

Sean O. Wilson
Ensign, United States Navy
B.S., North Carolina State University, 2001

Submitted in partial fulfillment of the
requirements for the degree of

**MASTER OF SCIENCE IN APPLIED PHYSICS**

from the

**NAVAL POSTGRADUATE SCHOOL**
**June 2002**

Author: Sean O. Wilson

Approved by: Bruce Denardo
Thesis Advisor

Andres Larraza
Second Reader/Co-Advisor

William B. Maier
Chairman, Department of Physics

THIS PAGE INTENTIONALLY LEFT BLANK

# ABSTRACT

Due to nonlinearity in the coupling, one of the vibrational modes of a straight symmetric triatomic molecule can be unstable for amplitudes greater than a threshold value. The instability is due to the mode parametrically exciting another mode. The threshold amplitude decreases if the difference of the frequency of the two modes is reduced. We consider the simplest case of a symmetric rectilinear molecule where the coupling has a cubic nonlinearity in addition to a linear restoring force. Approximate analytical results are in good agreement with numerical simulations of the exact equations of motion, although in some cases the actual behavior fundamentally deviates from the perturbative theory. Two physical demonstrations of the instability are described, where the apparatus are a system of gliders coupled by springs and magnets on an air track. Possible quantum mechanical implications are discussed. This work is a fundamental generalization of the parametric instability of two linearly coupled nonlinear oscillators that was reported in a previous investigation.

THIS PAGE INTENTIONALLY LEFT BLANK

# TABLE OF CONTENTS

THIS PAGE INTENTIONALLY LEFT BLANK

# LIST OF FIGURES

# SYMBOL GLOSSARY

a, parametric drive amplitude or length between end of M glider and center of m glider.
A, amplitude
b, length from center of m glider to attachment point of spring on transverse rail.
c, length of unstreatched spring.
$f_r$, response frequency.
$f_d$,drive frequency.
F, restoring force.
m, small (outer) masses of the triatomic molecule.
M, large (central) mass of the triatomic molecule.
t, time
x, direction of translational movement of triatomic molecule.
$x_1$, direction of movement for the small (outer) left mass.
$x_2$, direction of movement for the small (outer) right mass.
$x_3$, direction of movement for the large (central) mass.
$\ddot{x}_1$, acceleration of the small (outer) left mass.
$\ddot{x}_2$, acceleration of the small (outer) right mass.
$\alpha$, nonlinear coefficient in the spring.
$\theta$, half angle formed by a and c in the slanted-spring glider demonstration at maximum amplitude.
$\varphi$, half angle formed by a and c in the slanted-spring glider demonstration at minimum amplitude.
$\kappa$, spring constant or linear coefficient .
$\rho$, mass ratio (m/M).
$\omega^2$, frequency ratio ($\omega_o^2 / \omega_1^2$)
$\omega_0^2$, resonant frequency (k/m).
$\omega_1$, natural frequency ($\gamma\omega_0^2$)
$\xi$, lower-frequency mode of x, $[(x_1 - x_2) / 2]$.
$\ddot{\xi}$, acceleration of the lower-frequency mode.
$\eta$, upper-frequency mode of x, $[(x_1 + x_2) / 2]$.
$\ddot{\eta}$, acceleration of the upper-frequency mode.
$\gamma$, convenient mathematical parameter that specifies the ratio of the masses in the system.
$\Omega^2$, natural frequency.
$\delta t$, change in time.
epsilon, perturbation of the mode at rest in numerical simulations.
criterion, the minimum amplitude above zero which indicates instability.
tmax, maximum time examined.

THIS PAGE INTENTIONALLY LEFT BLANK

## ACKNOWLEDGMENTS

It is my pleasure to acknowledge my wife, who is also my closest friend and dearest companion. Your love and dedication are the foundation upon everything that may be judged as my success. You have stood patiently by my side for nearly a decade while I've spent nearly all our family hours in pursuit of knowledge. Thank you for believing in me and encouraging me to follow my dreams. My daughter, for the inspiration I gain watching you radiate a love for life that is unequaled in the smile or the eyes of any other.

I would like to thank the faculty of the NPS Physics department, especially my advisor, Professor Bruce Denardo. You kept me on course and taught me the real meaning of research.

Finally, I would also like to thank the staff of the NPS Physics department. Above all, Mr. George Jaksha, without his efforts my demonstrations never would have seen the light of day.

THIS PAGE INTENTIONALLY LEFT BLANK

# I. INTRODUCTION

The straight (often called linear) symmetric triatomic molecule is a well known and well understood system that is used as an example in intermediate (Fowles)(Marion) and graduate-level (Goldstein)(Landau) mechanics textbooks in determination of the normal longitudinal modes of a system, see Fig. 1. This system is known to have three longitudinal modes that we refer to as the zero-frequency mode, lower-frequency mode and upper-frequency mode. The zero-frequency mode corresponds to the rigid translation of the molecule along the longitudinal axis with constant velocity. The lower-frequency mode corresponds to the center mass remaining stationary while the end masses oscillate in opposite directions with the same amplitude and angular frequency $\omega_0 = (k/m)^{1/2}$. The upper-frequency mode corresponds to the outer masses oscillating in phase and with equal amplitudes while the center mass oscillates in antiphase with angular frequency $\omega_1 = (1 + 2m/M)^{1/2}\omega_0$ and amplitude scaled by the factor 2m/M. This corresponds to zero displacement of the center mass.

Previous work dealt with a system of two linearly coupled nonlinear oscillators, for which it was shown that one of the two normal modes is subject to the parametric instability. (Denardo) It was thought that a mode of a system would be subject to the principal parametric instability only if its frequency were twice the frequency of another mode. The investigation opened the possibility for parametric instabilities under conditions that may more readily occur because the instability is favored (i.e., the amplitude threshold is lower) when the frequencies of the two modes are near each other. This instability may have consequences regarding actual molecules (see below).

In contrast to previous work, this system does not deal with coupled oscillators. Rather, the nonlinearity exists in the coupling of the masses. The overall common characteristic between this system and the previous one is that the nonlinearity causes the normal modes to be coupled. Additionally, the instability is favored when the frequencies of the two normal modes are near each other, which occurs for $M >> m$ in the triatomic molecule.

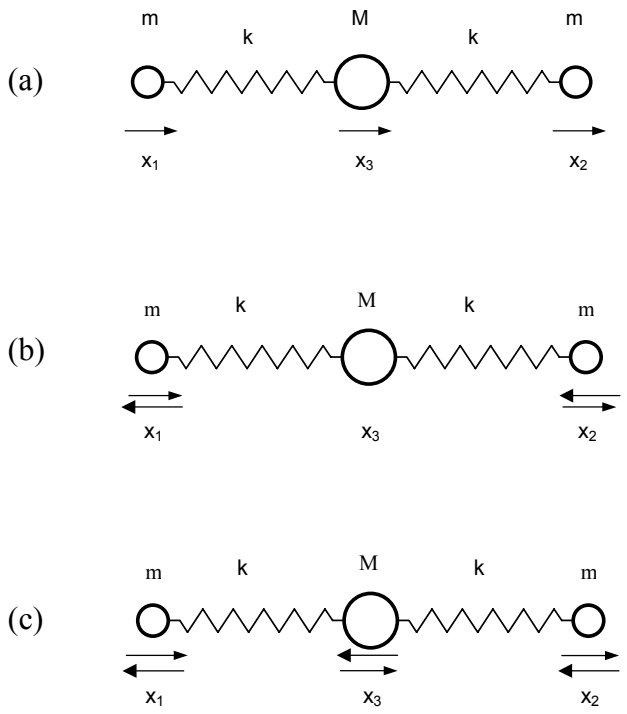


Figure 1. Symmetric rectilinear triatomic molecule, with outer masses m, central mass M, and spring constants k: (a.) translational motion (b.) lower-frequency motion (c.) upper-frequency motion.

This thesis shows that the nonlinearity in the coupling causes one of the two oscillatory normal modes to be unstable for amplitudes above a threshold value. The instability leads to a beating motion where energy is transferred back and forth between the lower and upper frequency modes. For simplicity, only a cubic nonlinearity in the displacement of each spring from equilibrium is assumed. The instability corresponds to the excited mode parametrically driving the other mode, which is referred to in general as *autoparametric resonance*. The instability is investigated analytically and numerically and two demonstration apparatus that exhibit the effect are described.

The motivation for this work is two-fold. First, the instability is an example of how nonlinearity in a system can lead to fundamentally different behavior. The instability is especially important in the case of a classical triatomic molecule, because this is a model system that is studied by nearly all physics students. Second, the existence of the (classical) instability raises interesting questions regarding the quantum mechanical behavior of an actual triatomic molecule, or, in general, any molecule that has

more than one vibrational mode. It is well known that the vibrational motion of molecules is nonlinear (Beiser), so the normal modes will be coupled. Although there is much literature on a broad variety of parametric excitation in quantum mechanical systems by external sources, (Quantum) we have not found any work on autoparametric resonance.

As a speculative example of a possible consequence for an actual triatomic molecule, consider a gas of such molecules. The unstable mode may not fully participate in the partition of energy among the degrees of freedom of the gas, so the specific heat would be *less* than the predicted value. This will occur if the temperature is sufficiently large such that average energy of the mode is roughly equal to or greater than the threshold value. For a cubic nonlinearity, we calculate the classical amplitude threshold in Secs. II.B and II.C.

As another speculative example, consider the case in which the ground state is classically unstable. As shown in Sec. II.A, this is possible for a softening cubic nonlinearity if M is sufficiently greater than m such that the amplitude threshold is less than the amplitude corresponding to the ground state energy. The instability cannot occur, because energy conservation would be violated. However, the classical instability may still have some manifestation, because it must occur at higher energies as a result of the correspondence principle. An example of a possible consequence is that, in the presence of photons or collisions, there may be an enhancement of the transition probability from the ground state to a state of the other mode.

We were initially motivated to investigate the parametric instability of a vibrational mode of a molecule because we thought that this could lead to a new type of laser; specifically, where a population inversion results fundamentally from the instability. However, the transition probability for absorption from one state to an excited state will still equal the transition probability for stimulated emission from the excited state to the original state, so it does not appear that the instability itself can give rise to a population inversion. However, an enhanced transition probability due to the instability could be beneficial in some lasers because it will cause the population inversion to occur more rapidly.

THIS PAGE INTENTIONALLY LEFT BLANK

# II. THEORY

## A. MODEL SYSTEM AND EQUATIONS OF MOTION

We consider longitudinal motion of the system shown in Fig. 1. The force, F, of each spring is generalized to include a cubic nonlinearity:

$$F = -kx + \alpha m x^3 \tag{1}$$

where x is the displacement of the spring from equilibrium, k is the spring constant, m is the mass of the outer masses and where the nonlinear coefficient $\alpha$ can be positive ("softening"), negative ("hardening"), or zero (linear). The factor of m in the cubic term is inserted only for mathematical convenience. The coupling force in actual molecules can be approximated by a sum of quadratic and cubic nonlinearities. We dealt with the simplest case, cubic nonlinearity.

The displacements of the masses are measured from points corresponding to equilibrium of the system. The equations of motion for the displacements $x_1$ and $x_2$ of the outer masses are

$$\ddot{x}_1 = -\omega_o^2 (x_1 - x_3) + \alpha (x_1 - x_3)^3 \tag{2}$$

$$\ddot{x}_2 = -\omega_o^2 (x_2 - x_3) + \alpha (x_2 - x_3)^3 \tag{3}$$

where the overdots denote differentiation with respect to time, and where $\omega_o^2 = k/m$. Because a possible uniform motion of the center of mass (zero-frequency normal mode) is irrelevant here, we employ the center-of-mass frame of reference. This reference frame reduces the number of degrees of freedom from three to two and the relationship among the displacements is $m(x_1 + x_2) + Mx_3 = 0$, so $x_3 = -\rho(x_1 + x_2)$, where $\rho = m/M$. Substituting this expression for $x_3$ into Eqs. (2) and (3) yields

$$\ddot{x}_1 = -\omega_o^2\left[(1+\rho)x_1 + \rho x_2\right] + \alpha\left[(1+\rho)x_1 + \rho x_2\right]^3 \qquad (4)$$

$$\ddot{x}_2 = -\omega_o^2\left[\rho x_1 + (1+\rho)x_2\right] + \alpha\left[\rho x_1 + (1+\rho)x_2\right]^3. \qquad (5)$$

Transforming Eqs. (4) and (5) to the linear normal mode coordinates $\xi = (x_1 - x_2)/2$ (lower-frequency mode) and $\eta = (x_1 + x_2)/2$ (upper-frequency mode) yields, after some simple algebra,

$$\ddot{\xi} + \omega_o^2\xi = \alpha\left(\xi^3 + 3\gamma^2\xi\eta^2\right) \qquad (6)$$

$$\ddot{\eta} + \omega_1^2\eta = \alpha\left(\gamma^3\eta^3 + 3\gamma\xi^2\eta\right) \qquad (7)$$

where $\omega_1^2 = \gamma\omega_o^2$, and where $\gamma$ is a mathematically convenient parameter that specifies the ratio of the masses: $\gamma = 1 + 2\rho = 1 + 2m/M$, which ranges from $\gamma = 1$ for $M = \infty$ to $\gamma = \infty$ for $M = 0$. The first limit corresponds to uncoupled oscillations of the m masses, while the second corresponds to the absence of M and thus a reduction to a single degree of freedom of vibration.

The square frequency of small-amplitude oscillations of the lower-frequency mode (normal coordinate $\xi$) is $\omega_o^2 = k/m$, while that of the upper-frequency mode (normal coordinate $\eta$) is $\omega_1^2 = \gamma\omega_o^2$. The equations of motion, Eqs. (6) and (7), for the normal modes are similar although not identical to those for the system of two nonlinear oscillators that are linearly coupled. (Denardo) The coupling stiffness between the two masses there plays the role of mass ratio $\rho = m/M = (\gamma - 1)/2$ here.

## B. LOWER-FREQUENCY NORMAL MODE

The analysis of the stability of each normal mode is similar to that in Ref. (Denardo). However, because the current case turns out to be more complicated, it is useful to alter the approach by first performing the graphical analysis and then the analytical analysis.

For the lower-frequency ($\xi$) mode, we consider weakly nonlinear oscillations $\xi = A\cos(\omega t)$, where $\omega$ and $A$ are constants. The relationship between the amplitude and frequency of these oscillations is approximately (Denardo)

$$\omega^2 = \omega_o^2 - \frac{3}{4}\alpha A^2 . \tag{8}$$

Substituting $\xi = A\cos(\omega t)$ into the $\eta$ equation of motion, Eq. (7), using the identity $\cos^2(\omega t) = [1 + \cos(2\omega t)]/2$, and neglecting the $\eta^3$ term because the amplitude of the $\eta$ motion is assumed to be small, gives

$$\ddot{\eta} + \left[ \omega_1^2 - \frac{3}{2}\gamma\alpha A^2 - \frac{3}{2}\gamma\alpha A^2 \cos(2\omega t) \right]\eta = 0 . \tag{9}$$

This has the form of the Mathieu equation $\ddot{\eta} + \left[\Omega^2 + a\cos(2\omega t)\right]\eta = 0$, for which it is known that parametric excitation occurs if the approximate threshold condition $|a| > 2|\Omega^2 - \omega^2|$ is met. (Denardo) A convenient graphical representation of this is to consider the drive plane of a vs. $\omega^2$. Parametric excitation occurs for all points inside the V formed by $a = \pm 2(\Omega^2 - \omega^2)$ in the upper-half plane. The vertex of the V has ordinate-intercept $\Omega^2$ and the lines have slope $\pm 2$, figure 2.

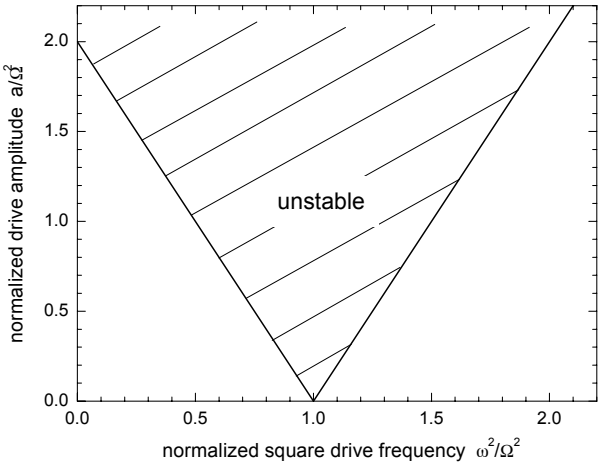


Figure 2. Graphical representation of the Mathieu equation for which the area inside the V represents the region for which parametric excitation occurs.

The parametric threshold condition $|a| > 2|\Omega^2 - \omega^2|$ corresponding to Eq. (9) is

$$\frac{3}{4}\gamma|\alpha|A^2 > \left|\omega_1^2 - \frac{3}{2}\gamma\alpha A^2 - \omega^2\right| . \qquad (10)$$

As in the case in Ref. (Denardo), an interesting fact is that Eq. (9) reveals that the frequency $\Omega$ is not independent of the drive amplitude a. That is, the linear frequency of the $\eta$ mode is altered by the finite amplitude oscillations of the $\xi$ mode. This has the effect of uniformly shearing the V in the plane of $|a|$ vs. $\omega^2$.

As in Ref. (Denardo), we conveniently unify the cases of softening ($\alpha > 0$) and hardening ($\alpha < 0$) by considering the plane of $\alpha A^2$ vs. $\omega^2$, where the ordinate can be positive or negative. The vertex of the sheared double V in the plane has ordinate-intercept $\omega_1^2$. The slopes of two lines of the double V can be determined from Eq. (10) by replacing the inequality with an equality, removing the two absolute values, and applying a $\pm$ sign to either side of the equation. The resultant values of the slopes are $-4/9\gamma$ and $-4/3\gamma$. A qualitative graph of the sheared double V is shown in Fig. 3.

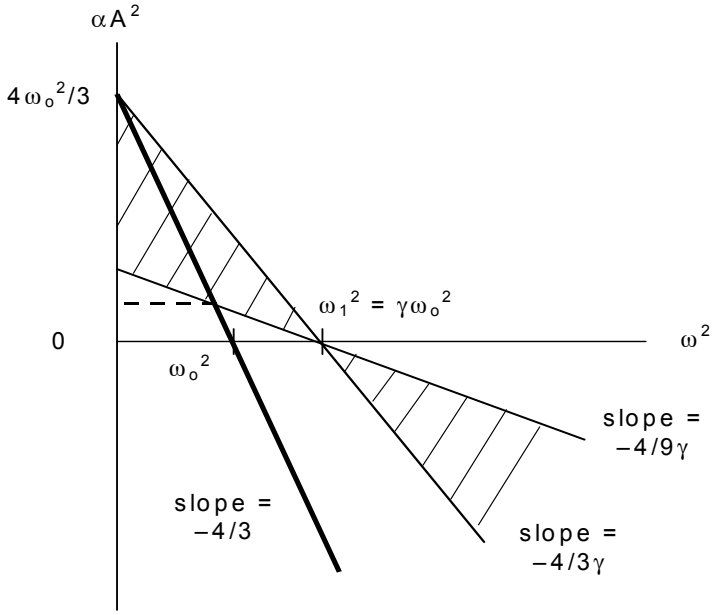


Figure 3. Qualitative sketch (not to scale) of the amplitude-frequency plane for parametric excitation of the upper-frequency (η) mode by the lower-frequency (ξ) mode with amplitude A, where $\gamma = 1 + 2m/M$. The excitation, and thus instability of the ξ mode, occurs for points on the heavy line that lie in the hatched region.

The ξ mode acts as a parametric drive on the η mode. The possible values of $\alpha A^2$ and $\omega^2$ are not independent, but are related by the amplitude-dependent frequency, Eq. (8), of the ξ mode. This corresponds to the line with ordinate-intercept $\omega_o^2$ and slope –4/3 (Fig. 3). The slope is steeper than the value $-4/3\gamma$ of the steeper of the two V lines, because $\gamma > 1$. A hardening ($\alpha < 0$) system is not subject to the instability, because the amplitude-dependent frequency line does not intersect the hatched region of the V. The softening results are in contrast to the previous case of two linearly coupled nonlinear oscillators, (Denardo) where the amplitude-dependent frequency and the steeper of the two lines of the V have the same slope, so there is a single threshold. In the current case, there is potentially both an upper and lower threshold. The instability is predicted to occur only for amplitudes between the two threshold values.

To calculate the two thresholds of the instability, we substitute the amplitude-dependent frequency, Eq. (8), into the parametric excitation condition, Eq. (10), replace the inequality with an equality, remove the two absolute values, and apply a ± sign to either side of the equation. The upper threshold value of the ordinate in Fig. 3 is then

found to be $\alpha A^2 = 4\omega_o^2/3$. According to Eq. (8), this corresponds to zero frequency, as shown in Fig. 3. Hence, according to our theory, there is a single threshold represented by the lower value. Parametric excitation of the $\eta$ mode occurs in the softening ($\alpha > 0$) case when the amplitude of the $\xi$ mode corresponds to a value above the dashed line in Fig. 3. The calculation of the lower threshold yields

$$\alpha A^2 \;>\; \frac{4}{3}\frac{\gamma-1}{(3\gamma-1)}\omega_o^2 \;=\; \frac{4}{3}\frac{\rho}{(1+3\rho)}\omega_o^2 \,, \qquad (11)$$

where we have recast the result in terms of the ratio of the masses $\rho = m/M = (\gamma - 1)/2$, which is more physically accessible. Because the energy of the $\xi$ mode must decrease if the $\eta$ mode is excited, Eq. (11) represents the amplitude threshold for instability of the $\xi$ mode. The theory predicts that the instability only occurs for a softening ($\alpha > 0$) system.

It should be noted that our calculations are based only on a leading-order perturbation theory. The lines in Fig. 3 are actually approximations to curves, so an upper threshold may exist for $\omega > 0$. The existence can be resolved by a higher-order perturbation calculation. An alternative, which we pursue in Ch. III, is to perform numerical simulations of the exact equations of motion, Eqs. (6) and (7).

## C. UPPER-FREQUENCY NORMAL MODE

The analysis of the stability of the upper-frequency ($\eta$) mode proceeds similarly to the $\xi$ mode in the previous section. However, in contrast to the system in Ref. (Denardo), the amplitude-dependent frequency of this mode is not the same as that for the $\xi$ mode. Rather, for weakly nonlinear oscillations $\eta = A\cos(\omega t)$, the equation of motion, Eq. (7), yields

$$\omega^2 = \omega_1^2 - \frac{3}{4}\gamma^3\alpha A^2 \,, \qquad (12)$$

which differs from that of the $\xi$ mode by a factor of $\gamma^3$ in the amplitude term, so the frequency shift is greater because $\gamma > 1$. This is due to the fact that, for a specified amplitude A of the two outer masses in the system (Fig. 1), the springs are stretched and compressed a greater amount for the upper-frequency mode than the lower-frequency mode, because M oscillates in antiphase in the first case and is motionless in the second case. It is easily shown that the amplitude of the spring oscillations is simply $\gamma A$. The slope of the line of the amplitude-dependent frequency, Eq. (12), in the plane of $\alpha A^2$ vs. $\omega^2$ is $-4/3\gamma^3$.

The equation analogous to Eq. (9) is

$$\ddot{\xi} + \left[ \omega_o^2 - \frac{3}{2}\gamma^2\alpha A^2 - \frac{3}{2}\gamma^2\alpha A^2 \cos(2\omega t) \right] \xi = 0 \ . \qquad (13)$$

This is identical to Eq. (9) if we let $\eta \to \xi$, $\omega_1 \to \omega_o$, and $\gamma \to \gamma^2$ in Eq. (9). Hence, the slopes of the sheared double V, which were $-4/3\gamma$ and $-4/9\gamma$ in the previous case, must now be $-4/3\gamma^2$ and $-4/9\gamma^2$. Furthermore, by the same replacements, the equation analogous to Eq. (10) must be

$$\frac{3}{4}\gamma^2 |\alpha| A^2 > \left| \omega_o^2 - \frac{3}{2}\gamma^2\alpha A^2 - \omega^2 \right| \ . \qquad (14)$$

The slope $-4/3\gamma^3$ of the amplitude-dependent frequency line of the $\eta$ mode from Eq. (12) is less steep than the slope $-4/3\gamma^2$ of the steeper line of the V, because $\gamma > 1$. Furthermore, the slope of the amplitude-dependent frequency line equals the slope $-4/9\gamma^2$ of the less steep line of the V when $\gamma = 3$. There are thus two possible cases, $\gamma < 3$ or $\gamma \geq 3$, which are shown in Figs. 4 and 5, respectively. Because $\gamma = 1 + 2m/M$, note that $\gamma < 3$ or $\gamma \geq 3$ corresponds respectively to simply $\rho < 1$ ($m < M$) or $\rho \geq 1$ ($m \geq M$).

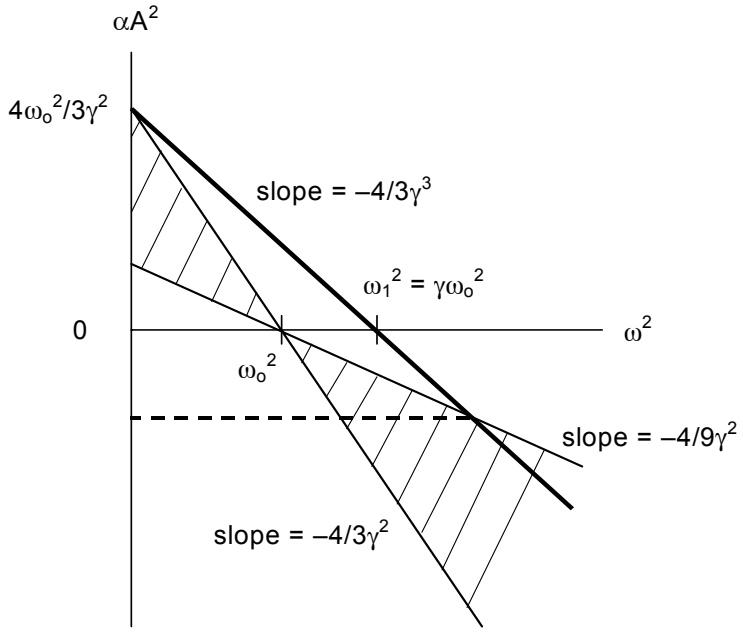


Figure 4. Qualitative sketch (not to scale) of the amplitude-frequency plane for parametric excitation of the lower-frequency (ξ) mode by the upper-frequency (η) mode with amplitude A. This case corresponds to m < M. The excitation, and thus instability of the η mode, occurs for points on the heavy line that lie in the hatched region.

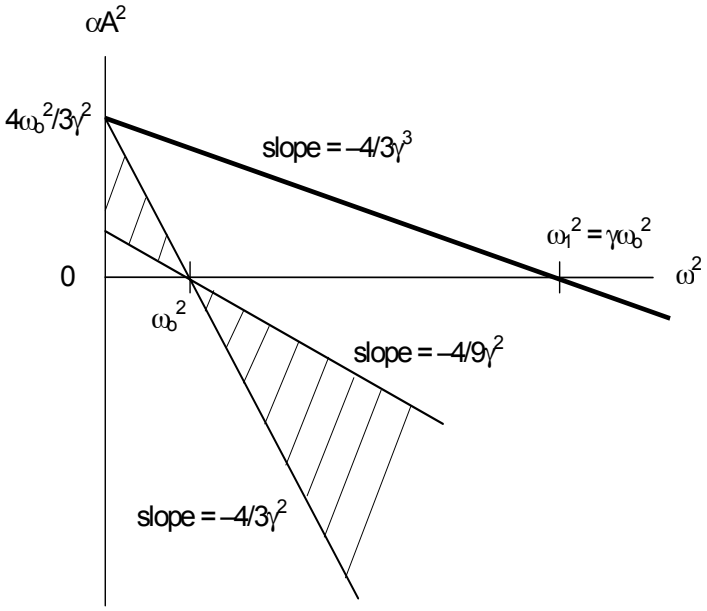


Figure 5. Qualitative sketch (not to scale) of the amplitude-frequency plane for parametric excitation of the lower-frequency (ξ) mode by the upper-frequency (η) mode with amplitude A. This case corresponds to m ≥ M (in contrast to m < M in Fig. 3). The excitation, and thus instability of the η mode, is not predicted to occur, because no points on the heavy line lie in the hatched region.

There is potentially an upper threshold in both cases. However, as in the previous case (Sec. II.B), this is shown below to correspond to $\omega = 0$, and so is predicted to have no effect. Due to the relative values of the slopes of the lines of the V and the amplitude-dependent frequency, a hardening ($\alpha < 0$) upper-frequency mode with amplitude greater than that corresponding to the dashed line in Fig. 4 is predicted to be unstable, which occurs only for $\gamma < 3$. For $\gamma \geq 3$, Fig. 5 shows that the mode is not subject to the instability.

To calculate the thresholds of the instability, we substitute the amplitude-dependent frequency, Eq. (12), into the parametric excitation condition, Eq. (14), and proceed similarly as in the previous case (Sec. II.B). The upper threshold value of the ordinate in Figs. 4 and 5 is then found to be $\alpha A^2 = 4\omega_o^2/3\gamma^2$, which corresponds to zero frequency according to Eq. (12). The theory thus predicts that this threshold does not exist. The calculation of the lower threshold in Fig. 4 yields the condition

$$-\alpha A^2 \; > \; \frac{4}{3}\frac{\gamma-1}{\gamma^2(3-\gamma)}\omega_o^2 \; = \; \frac{4}{3}\frac{\rho}{(1+2\rho)^2(1-\rho)}\omega_o^2 \,, \qquad (15)$$

which is valid for $\gamma < 3$ or $\rho < 1$. The theory thus predicts that a hardening ($\alpha < 0$) upper-frequency mode is unstable for amplitudes that satisfy Eq. (15), and that a softening ($\alpha > 0$) upper-frequency mode is not subject to the instability.

As in the previous case, the results are based only on a leading-order perturbation theory. The lines in Figs. 4 and 5 are actually approximations to curves, so an upper threshold may exist for $\omega > 0$. We resolve this with numerical simulations in Ch. III.

THIS PAGE INTENTIONALLY LEFT BLANK

# III. NUMERICAL SIMULATIONS

Numerical simulations of the exact equations of motion, Eqs. (6) and (7), were run utilizing Microsoft Visual Studio 1999 in the C++ programming language. To view programs, see Appendix A. Both the upper-frequency mode, $\eta$, and lower-frequency mode, $\xi$, were examined in both the hardening and softening nonlinear cases. Dimensionless units were used where $\omega_0 = 1$ and $\alpha = \pm 1$. All simulations were performed using the Euler-Cromer method. (Garcia) To determine the stability of each mode in the simulation where the maximum amplitude was unity, the mode under investigation was given an initial amplitude and the other mode was perturbed. The perturbation amplitude, epsilon, ranged from 0.001 to 0.00001, time steps ranged from $\delta t = 0.01$ to 0.0001 and the maximum time examined ranged from $t_{max} = 100$ to 5000. Time series were imported into Microcal Origin 6.0 and plotted for observation. Due to a decreasing period of motion for larger amplitudes in a hardening system, a sufficiently small time step had to be used to ensure that a false instability was not documented. An example of this is the hardening upper-frequency mode (Sec. III.D) for $\rho = m/M \geq 1$, which we originally found to be unstable above an amplitude threshold, but which we later realized was a numerical artifact due to the time step being too large. The criterion for determining stability was a 0.001 increase in the amplitude of the zero amplitude mode. In agreement with the theory, only the hardening upper-frequency mode and the softening lower-frequency mode displayed the parametric instability.

Additionally, each softening mode was examined for the point at which the motion would diverge if the system were provided enough energy to exhibit "over-the-top" motion. This can be viewed similar to a ball in a valley with peaks on either side. If given to much energy, the amplitude of oscillation will exceed the height of one of the peaks and the ball will roll over the peak and never return. We call this the "over-the-top" amplitude, $A_{OTT}$.

## A. SOFTENING LOWER-FREQUENCY MODE

In the lower-frequency mode, the case where the coupling softens is predicted by the theory to be parametrically unstable. When the lower-frequency mode is initiated with great enough amplitude, the system demonstrates a beating motion where energy is transferred from one mode to the other (Fig. 6). The nonlinearity causes the initially-excited mode to parametrically drive the other mode at twice the frequency of the initially-excited mode, as seen in Eq. (9). This is known as the *principal parametric resonance*, where the frequency of the response locks onto one-half the frequency of the drive, and is the basis of our theory. In the general theory of parametric excitation, see references in Ref. (Denardo), it is shown that there occur other resonances in which the ratio of the response to drive frequency is 1 (isochronous resonance), 3/2, 2, 5/2, etc., although these are successively more difficult to obtain.

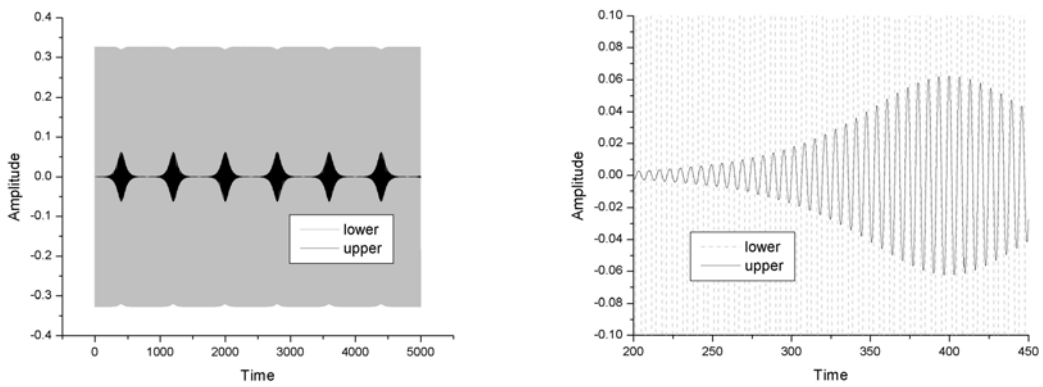


Figure 6. (a) Unstable oscillation repeating in the lower-frequency mode (gray lines) with softening nonlinearity for $\rho = 0.1$, $A = 0.3267$ and criterion = 0.001. Space between oscillations is so small that oscillations appear as gray background. Starting amplitude is 2% greater than the amplitude threshold for this system. (b) Magnification of (a) to show the increasing amplitude in the upper-frequency mode.

When the initial amplitude of the lower-frequency mode is decreased, the resultant amplitude of the upper-frequency mode is also decreased. Additionally, the time required for the peak to occur in the upper-frequency mode increases (Fig. 7). As the amplitude threshold is approached, the peak amplitude of the upper-frequency mode approaches zero and the time increases to infinity. Thus, it may appear impossible to accurately determine the amplitude threshold. However, sufficient accuracy on the scale of Fig. 8 (see below) is not difficult to obtain.

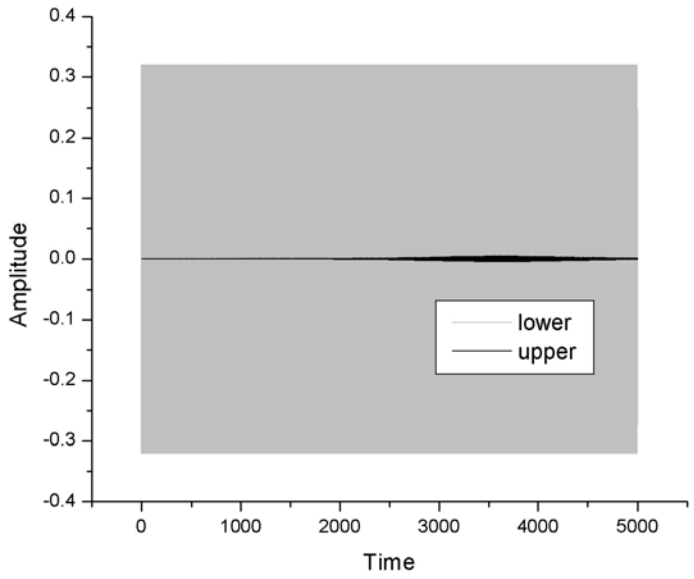


Figure 7. Unstable oscillation in the lower-frequency mode (gray lines) with softening nonlinearity for $\rho$ = 0.1, A = 0.3204 and criterion = 0.001. Space between oscillations is so small that oscillations appear as gray background. The threshold amplitude for this system is $A_{th}$ = 0.3203.

The dependence between the threshold amplitude for the parametric instability and the mass ratio of the system can be seen in Fig. 8. As the mass ratio increases, so does the amplitude threshold. The theory is only expected to be valid when the frequencies of the normal modes are near each other, which corresponds to $\rho << 1$. The circles correspond to the amplitude threshold found through numerical simulation for values of $\rho$ ranging from 0.01 to 2. These values are plotted against equation (11) and are in good agreement for $\rho < 0.98$. However, at $\rho \approx 0.98$ the system no longer appears to exhibit the instability but goes straight into "over-the-top" motion given great enough amplitude. This is in sharp contrast to the theoretical over-the-top amplitude of 1.

Figure 8 also shows the amplitude threshold for divergent (unbounded) motion. For amplitudes between the circles and the squares the parametric instability leads to the increasing beating amplitudes and increasing beating frequency described above. The divergent motion can occur because the coupling force, Eq. (1), for $\alpha > 0$ corresponds to a potential energy that is a well only for $|x| < (k/\alpha m)^{1/2} = \omega_0 \alpha^{1/2}$, and negatively diverges as $|x| \rightarrow \infty$. The central mass M is at rest for the lower-frequency normal mode, so the

expected amplitude threshold for this "over-the-top" instability is simply $\omega_0\alpha^{1/2} = 1$ (in dimensionless units). The data in Fig. 8 show that the parametric instability causes over-the-top motion to occur for amplitudes that are substantially less than the expected value, unless $\rho << 1$. This behavior is not yet understood, and is in contrast to the case of linearly coupled nonlinear oscillators. (Denardo) For $\rho \geq 1$, the parametric instability at the amplitude threshold initiates the over-the-top motion, to at least three significant figures in the value of the amplitude.

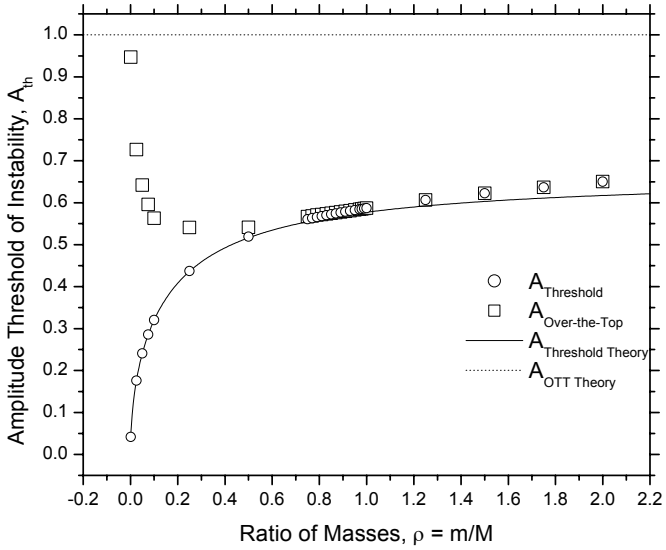


Figure 8. Deviation between the theoretical calculation and the numerical simulation results for the threshold amplitude of the lower-frequency mode with softening nonlinearity. Additionally, the "over-the-top" amplitude approaches the threshold amplitude and dominates at $\rho \geq 1.0$. $A_{th} = A_{threshold}$

Data was gathered for values of $\rho$ beyond those in Fig. 8, and discontinuities in the threshold amplitude as a function of $\rho$ were found (Fig. 9). The first discontinuity is at $\rho = 3.0$, where the threshold amplitude jumps from 0.71 to 0.53 as $\rho$ is increased. The second is at $\rho = 7.1$, where the jump is from 0.64 to 0.54. Examination of time series reveals that the first discontinuity corresponds to the isochronous parametric resonance. This continues to occur until the next discontinuity, which corresponds to the 3/2 parametric resonance. For this range of $\rho$ values, the principal parametric resonance

presumably continues to exist, but the threshold for the isochronous resonance is smaller. There is apparently an infinite sequence of discontinuities that corresponds to the sequence of parametric instabilities described above. For examples of the sequence of parametric instabilities see Appendix B.

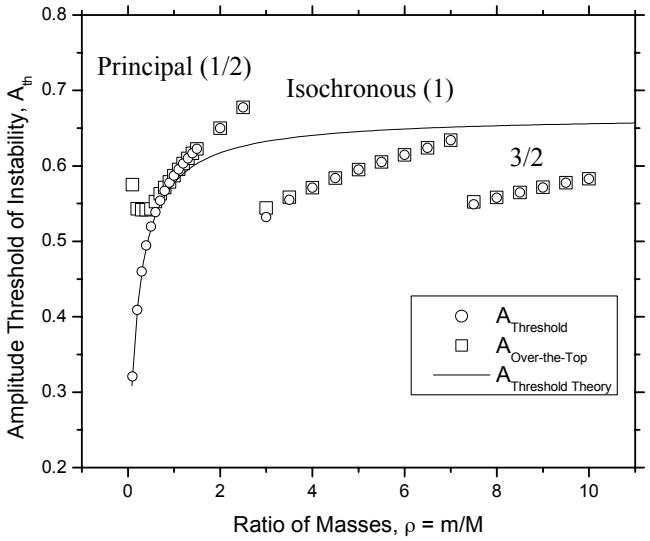


Figure 9. Instabilities due to higher order parametric resonances in the lower-frequency softening mode at high values of ρ. $A_{th} = A_{threshold}$

In Sec. II.B, the possibility was mentioned of an upper threshold existing for $\omega > 0$ due to the lines in Fig. 3 being approximations to curves. However, numerical simulation showed no such threshold for $0 < \rho < 1$. The instability may be prevented by the presence of the over-the-top instability of our model force, Eq. (1). Other softening forces that do not possess this property may yield an upper threshold. An example is the force whose potential energy in dimensionless units is $\ln(1+x^2)$.

## B. HARDENING LOWER-FREQUENCY MODE

The theory also predicts that the hardening lower-frequency mode should be stable for the parametric instability. Numerical simulations show that this mode is stable for $\rho < 0.5$, except at $\rho \approx 0$ due to the curve approximation of Fig. 3. For $0.5 \leq \rho \leq 1.2$, the system enters a region of instability which examination of the time series shows is

caused by the isochronous parametric resonance, App. B. The instability repeats for 2.0 $\leq \rho \leq$ 3.1 and 4.1 $\leq \rho \leq$ 5.0. Examination of the time series showed that these regions were the 3rd and 4th order parametric resonances, respectively. Thus, we were able to isolate the regions of 1st through 4th order parametric resonance between $0 < \rho \leq 5$, see Fig. 10. The figure clearly shows regions of stability between regions of instability. It appears that as $\rho$ is increased, successive higher-order parametric resonances occur over intervals that are separated by intervals of stability. Care had to be taken in ensuring the time steps were low enough that no significant change occurred in the motion between time steps. It should be noted that "over-the-top" motion is not possible for a hardening nonlinearity.

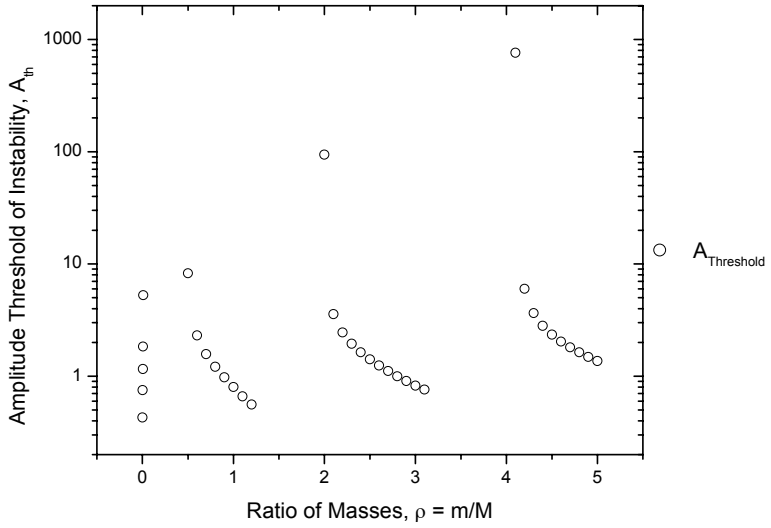


Figure 10. Mass dependence on the amplitude threshold of the lower- frequency mode with hardening nonlinearity.

As mentioned in Sec. (II.B), the possibility exists for a region of instability near $\rho \approx 0$, because the lines in Fig. 3 are actually approximations to curves. Numerical simulations show that for $0.001 \leq \rho \leq 0.009$ the instability does exist, see Figs. 10 and 11. The amplitude threshold increases monotonically from zero as $\rho$ increases, and has the value 1.1591 at $\rho = 0.005$.

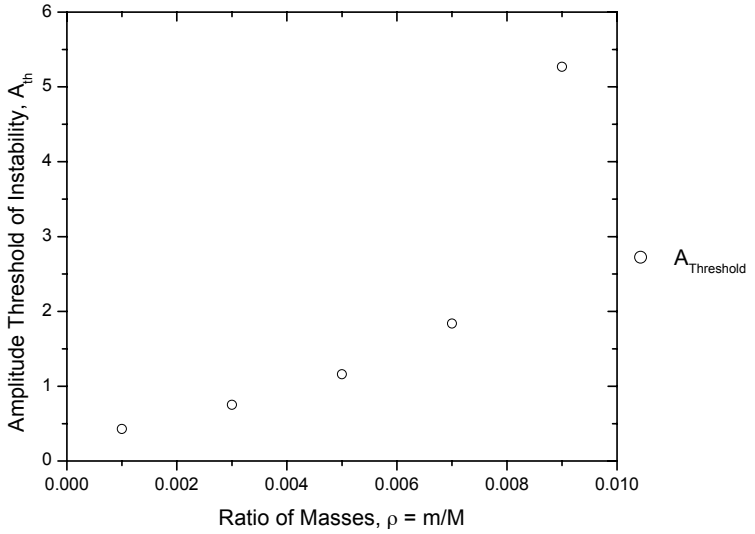


Figure 11. Threshold amplitude for the lower- frequency mode with hardening nonlinearity at low ρ values.

## C. SOFTENING UPPER-FREQUENCY MODE

According to the theory in Sec. II.C, the upper-frequency mode with softening nonlinearity was predicted by theory not to be subject to the parametric instability. Additionally, over-the-top motion should occur when the change in length of a spring exceeds the value corresponding to zero force in Eq. (1), which is $\omega_0/\alpha^{1/2}$. For the upper-frequency mode with amplitude A, the central mass M moves in antiphase with amplitude $2\rho A$, so the change in length of a spring is $(1 + 2\rho)A = \gamma A$. The theoretical maximum stable amplitude of the upper mode is thus $\eta_{max} = \omega_0/\gamma\alpha^{1/2} = 1/\gamma$ (in dimensionless units).

However, numerical simulations revealed growth in the lower mode for $0 < \rho < 0.017$, and over-the-top motion for all values of ρ (Fig. 12). However the "over-the-top" amplitude was 10-20% less than the theoretical value, depending upon the value of γ unless $\gamma \approx 1$ ($\rho \approx 0$). The discrepancy persists even when we make the amplitude of the perturbation of the lower mode extremely small.

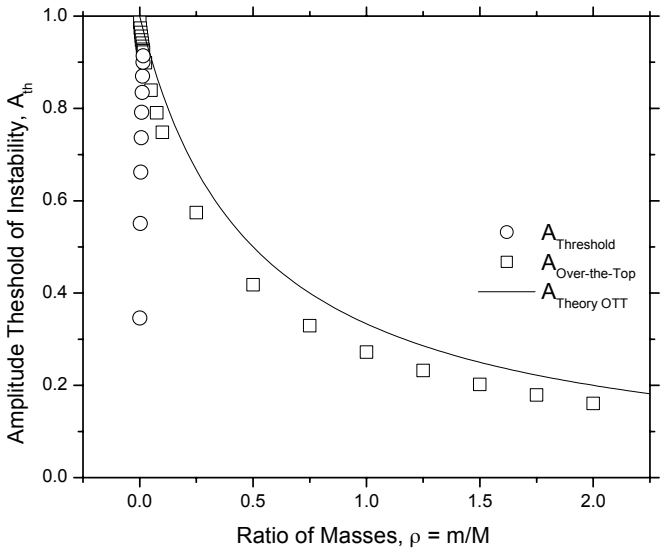


Figure 12. Amplitude threshold for the upper-frequency mode with softening nonlinearity $A_{th} = A_{threshold}$.

Zooming into the point of initial perturbation shows isochronous resonance and continuous increase in the amplitude of the lower-frequency mode until the system exhibits over-the-top motion (Fig. 13). When this happens, the upper-frequency mode exhibits over-the-top motion as well. The direction of increasing amplitude, positive or negative, depends on the direction of perturbation. The interesting point to note is that the amplitude of the lower mode never goes below the value of the perturbation it received, it either stays at values greater than 0.0001 or less than –0.0001 (Fig. 14). Thus, it appears that the isochronous parametric resonance is responsible for initiating the over-the-top motion. This instability of the softening upper mode is in contrast to the previously investigated case of two linearly coupled nonlinear oscillators, (Denardo) for which it was found that the mode was stable for all amplitudes less than the theoretical over-the-top amplitude.

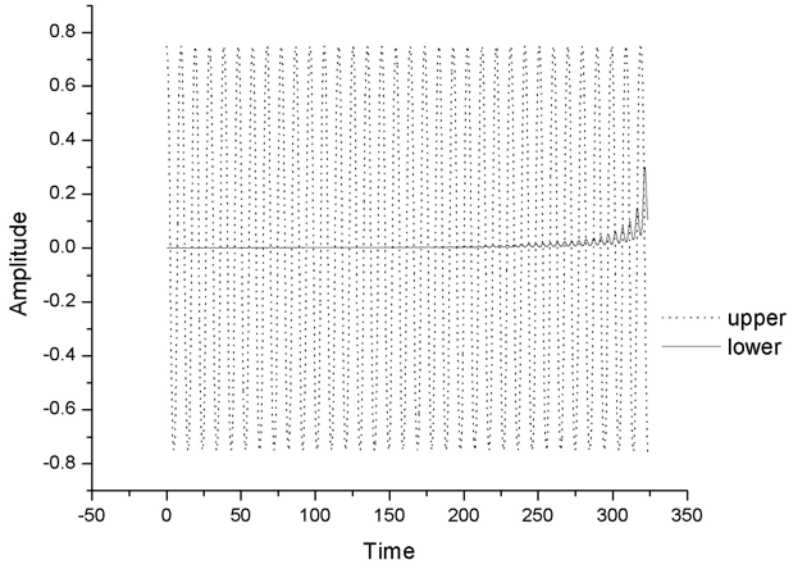


Figure 13. "Over-the top" motion in the upper-frequency mode with softening nonlinearity.

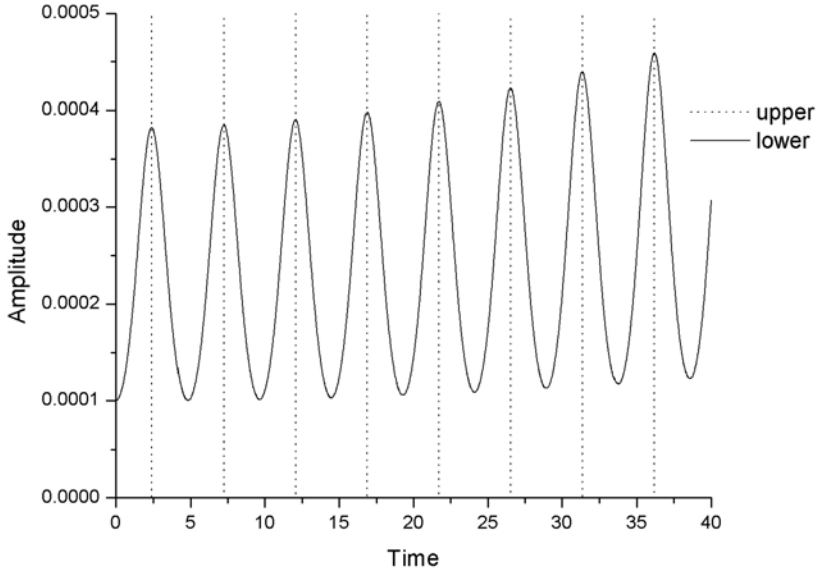


Figure 14. Zoom of "over-the-top" motion in the upper-frequency mode with softening nonlinearity

As explained in Sec.- II.C, when $\rho \approx 0$ there is a possibility of a threshold amplitude above which the softening upper-frequency mode may be subject to the principal parametric instability. Numerical simulations show that this does occur for

$0 < \rho \leq 0.016$ (Fig. 15). The amplitude threshold increases monotonically from zero as $\rho$ increases, and has the value 0.662 at $\rho = 0.005$. The threshold smoothly connects with the isochronous resonance threshold at $\rho = 0.017$. For $\rho$ not near zero, the existence of principal parametric resonance cannot be resolved due to the presence of the over-the-top instability of our force model, Eq. (1), as in the case of the softening lower-frequency mode (Sec- III.A)

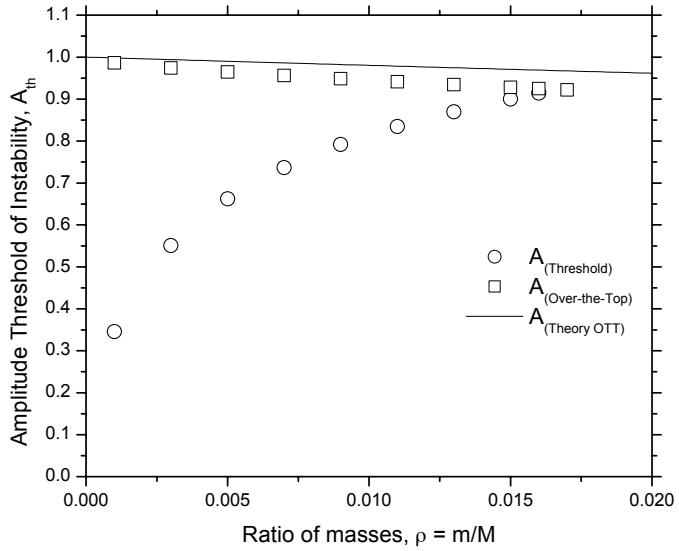


Figure 15. Amplitude threshold for the upper-frequency mode with softening nonlinearity in the region of $\rho \approx 0$. $A_{th} = A_{threshold}$.

## D. HARDENING UPPER-FREQUENCY MODE

In the case where the coupling hardens, the theory in Sec. II.C predicts the upper-frequency mode to be unstable for the parametric instability for amplitudes above the threshold value given by Eq. (15) for $0 < \rho < 1$, and to not exhibit the instability for $\rho \geq 1$. As with the lower-frequency mode with softening nonlinearity, when the upper-frequency mode is initiated with great enough amplitude, the system demonstrates the same beating motion where the frequency of the two modes is the same and is consistent with the principal parametric resonance (Fig. 16). The greater the amplitude above threshold, the higher the repetition frequency.

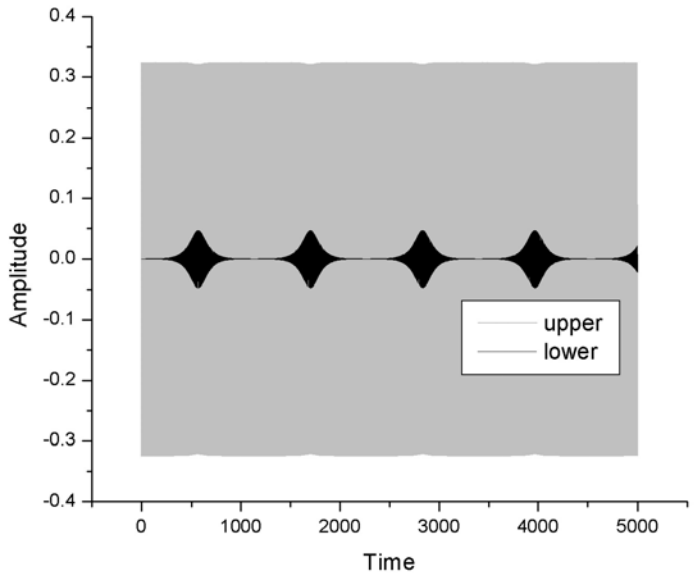


Figure 16. Unstable oscillation repeating in the upper-frequency mode (gray lines) with hardening nonlinearity for $\rho = 0.1$, $A = 0.3241$ and criterion = 0.001. Space between oscillations is so small that oscillations appear as gray background. Starting amplitude is 1% greater than the amplitude threshold for this system.

Numerical simulations of the exact equations of motion, Eqs. (6) and (7), identified the instability with increasing amplitude of the lower-frequency mode from zero, as seen in Fig. 17. When the initial amplitude of the upper-frequency mode is decreased, the resultant amplitude of the lower-frequency mode is also decreased. Additionally, the time required for the peak to occur in the lower-frequency mode also increases. As the amplitude threshold is approached, the peak amplitude of the upper-frequency mode approaches zero and the time increases to infinity.

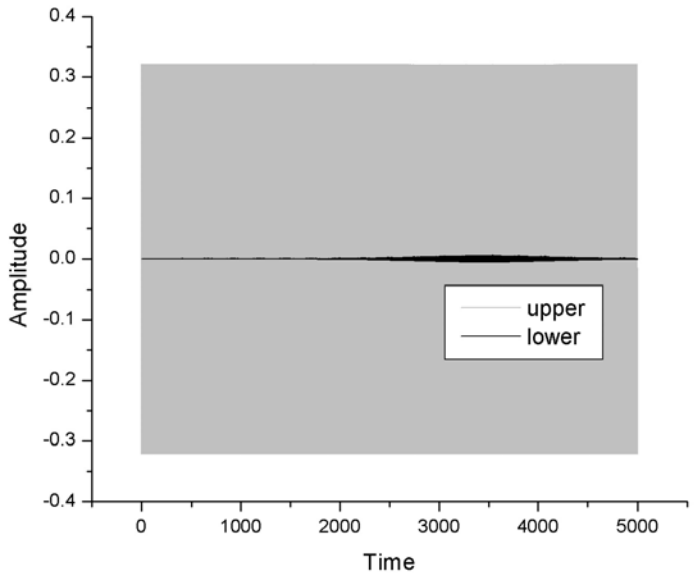


Figure 17. Unstable oscillation in the upper-frequency mode (gray lines) with hardening nonlinearity for $\rho$ = 0.1, A = 0.3209 and criterion = 0.01. Space between oscillations is so small that oscillations appear as gray background. The threshold amplitude for this system is 0.3208.

The dependence between the threshold amplitude and the mass ratio can be seen in Fig. 18. As the mass ratio increases, so does the amplitude threshold. The amplitude threshold was found through numerical simulations for $0 < \rho < 1$. The system did not exhibit the instability for $1 \leq \rho \leq 2$. The experimental values were plotted against Eq. (15) and are in good agreement for $\rho < 1$, even at $\rho = 0.999$ where the approximate analytical amplitude threshold is only 1.3% less than the numerical simulation value.

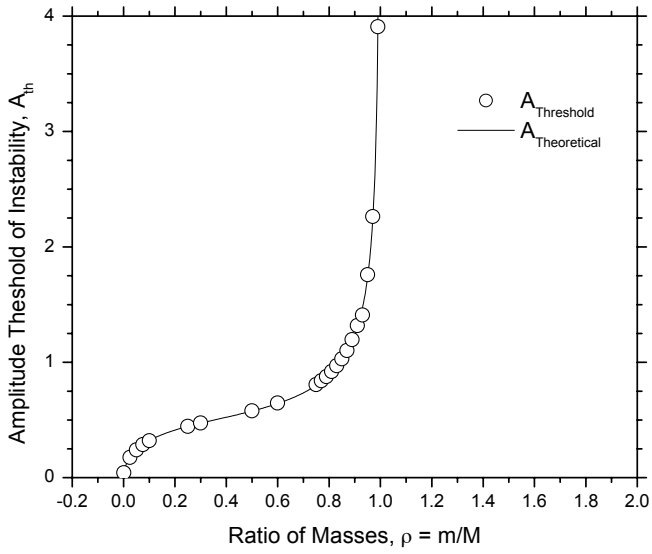


Figure 18. Theoretical calculation and the numerical simulation results for the threshold amplitude of the upper-frequency mode with hardening nonlinearity. $A_{th} = A_{threshold}$.

Based on our experience with the previous mode (Sec.- III.A), we expected the parametric resonances other than the principal resonance would occur for $\rho \geq 1$. This is apparently not the case, however, because numerical simulations for a wide variety of mass ratio and amplitude values yield a stable upper-frequency mode, as long as the time step is chosen to be sufficiently small.

As explained in Sec.- II.C, the hardening upper-frequency mode for $\rho \approx 0$ may become stable above an upper amplitude threshold. However, numerical simulations show no evidence of this.

THIS PAGE INTENTIONALLY LEFT BLANK

# IV. DEMONSTRATIONS

## A. THREE COUPLED PENDULUM SYSTEM

For a visual example of the two linear normal oscillatory modes and the instability of the triatomic molecule, the triatom system was translated into a three-coupled pendulum system, see Fig. 19. This system is similar to the two-coupled-pendulum system apparatus discussed in Ref. (Denardo). This system has three linear normal modes. In the fundamental normal mode, all three pendulums oscillate in phase with the same amplitude. The two other linear normal modes are similar to the two oscillatory normal modes of the triatomic molecule, the lower and upper modes. There is a distinction between the fundamental mode of the pendulum system and the zero-frequency mode of the triatomic molecule, but this is irrelevant in regard to the oscillatory modes of the triatomic molecule. There is also a distinction in the nonlinearity of the two systems. The pendulums are coupled nonlinear oscillators, whereas the triatomic molecule is a system of nonlinearly coupled masses.

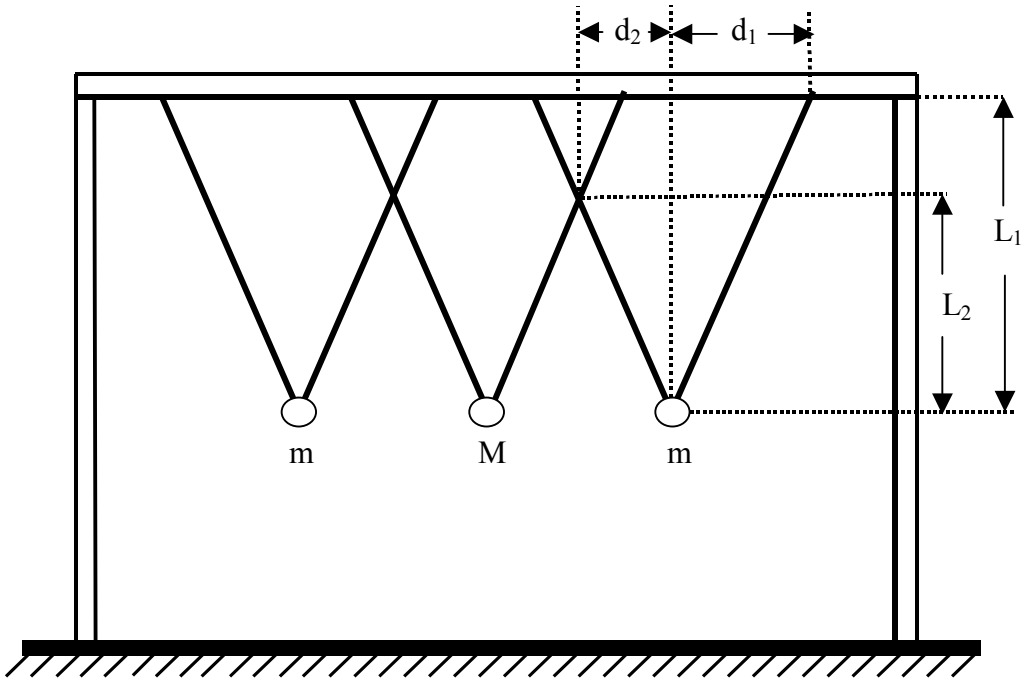


Figure 19. Three-coupled pendulum system where the center mass is heavier than the outer masses.

Pendulums #1 & #3 were of equal size and weight, m = 39.5 g. For pendulum #2, aluminum, brass and lead weights were used. Pendulum #2 was $m_{Al}$ = 79.3 g, $\rho_{Al}$ = 0.498, $m_b$ = 246.2 g, $\rho_b$ = 0.161, and $m_{Pb}$ = 302.1 g, $\rho_{Pb}$ = 0.131. The distance from the center of the large V is $d_1$ = 12 cm. The distance from the center of the small V is $d_2$ = 22 cm. The length of the large V is $l_1$ = 39.5 cm. The length of the small V is $l_2$ = 10 cm. The aluminum weight was employed in the lower and upper frequency modes at low and high amplitudes and all four variations of the system were stable. The same was true for the brass and lead weight system. This is perhaps not surprising because the nonlinearity of the two systems is different (see above). However, we did find that the fundamental mode of the three-pendulum system is unstable above an amplitude threshold. This is the few-degree-of-freedom limit of the Benjamin-Feir instability in continuous systems. (Denardo)

## B. MAGNASWING

Next, due to its similarity to the triatomic molecule, the commercial MagnaSwing™ toy (Denardo) was investigated using three magnetic pendulums set to repel one another (Fig. 20). As sold, this is a system of as many as five pendulums that oscillate longitudinally, where magnets in the bobs supply the coupling. As in the above system of coupled pendulums, the fundamental mode is distinct from the zero-frequency mode of the triatomic molecule, but this is irrelevant. This system does display two other modes which are similar to the upper and lower frequency modes of the triatomic molecule system.

Additionally, the nonlinearity is distinct from the triatomic molecule not only as a result of the pendulum nonlinearity, but also because the magnetic coupling is modeled by both cubic and quadratic nonlinearities in the force. Our theory (Secs.- II.B and II.C) assumes a pure cubic nonlinearity. It is thus perhaps not surprising that the two modes that are similar to the triatomic oscillatory modes did not exhibit the instability. The pendulums were all of equal size (d= 32 mm) and weight (m = 41.9 g). The center pendulum was weighted with a solid brass cylinder (d = 30.75 cm, m = 106.1 g) to achieve a mass ratio of $\rho$ = 0.284. As in the coupled pendulum system, even with a substantially increased central mass, the instability still did not occur. The lower mode of

vibration was stable at all amplitudes. The upper mode of vibration, though difficult to find, was also stable at all amplitudes.

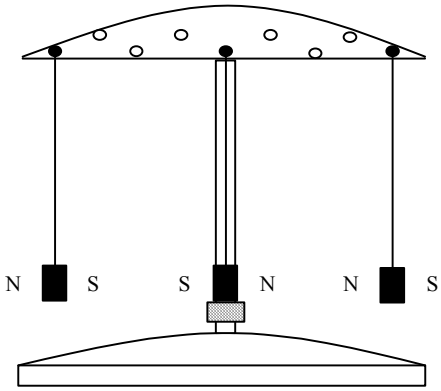


Figure 20. A three-pendulum configuration of the MagnaSwing toy. The pendulums were all the same size and weight and additional solid brass weight was added to the center pendulum to achieve a mass ratio of 0.284.

## C. HARDENING AIR TRACK GLIDER SYSTEM (MODEL 1)

The third system I investigated was three coupled gliders on an air track (Fig. 21). The gliders were connected by two springs (one on each side to maintain symmetry) and mounted with repulsive ceramic magnets. The purpose of the magnets was to introduce a hardening nonlinearity. This system is identical to the triatomic model with the exception that the coupling can be approximated by both quadratic and cubic nonlinearities, whereas the model assumes a pure cubic nonlinearity. The mass of the magnets was between 47.7 g and 49.0 g. Each glider was weighed and multiple combinations of magnets were used to ensure gliders #1 & #3 were always of the same weight. Multiple variations of this system were examined using gliders with mass 150 g, 300 g and 400 g. Mass ratios between 0.269 and 0.8 were achieved. Neither of the oscillatory normal modes were found to exhibit the instability, even at large amplitudes and small mass ratios.

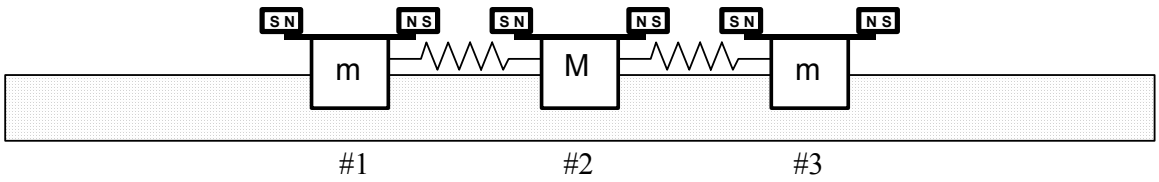


Figure 21. Air track glider setup to mimic the longitudinal vibration of a triatomic molecule using three spring coupled gliders and ceramic magnets.

In the demonstrations described so far, it should be noted that the lower-frequency mode can be readily excited by releasing the outer masses simultaneously from rest at the same amplitude in opposite directions, with the central mass at rest. In the first two demonstrations, pure upper-frequency mode motion can be difficult to excite by attempting to release the masses with the proper relative amplitudes. An alternative is to use a finger to drive a mass or, in the case of a pendulum, a point near the pivot. By resonantly driving one of the masses at the frequency of the upper mode, patiently waiting for transient motion to sufficiently decay, and carefully removing the drive, an approximately pure upper mode can be obtained. In the third demonstration, as well as the demonstrations below, the upper-frequency mode is easily excited by simply holding M at rest and displacing the two m's the same distance in the same direction, and simultaneously releasing all the masses from rest. As long as the system is symmetric, this initial condition excites only the upper-frequency mode.

Although none of the above four systems exhibit the desired instability, it should be noted that each of these apparatus offers an easy means of demonstrating the two linear normal oscillatory modes of the triatomic molecule. This is useful in the classroom because it offers a concrete visualization of the motion.

## D. HARDENING AIR TRACK GLIDER SYSTEM (MODEL 2)

Our failure with the quick demonstrations described above prompted us to build apparatus with symmetric potential wells, for which the theory in Secs.- IIB and II.C is an approximation due to the cubic correction to a linear force. In contrast to the simple apparatus for the previously-investigated instability of two linearly coupled nonlinear oscillators, (Denardo) the apparatus here require much more effort to construct. Figure 22 shows a system with an air track, gliders, springs and magnets that are realizations of a classical triatomic molecule with symmetric nonlinear potentials. The nonlinearity of the apparatus is due to the repulsive forces of the magnets, and the outer magnets on the outer gliders are for balance only, in order to minimize friction. We use strong ceramic magnets of diameter 2.2-cm and length 2.5-cm. The magnets are taped to 7.5-cm long channels made by cutting PVC pipe lengthwise in half. The channels are attached to the gliders with screws. In this system the upper-frequency mode should be unstable as long

as $\rho = m/M < 1$. The outer-most gliders were added to the ends of model 1 and connected by a 1.9 cm diameter and 152.4 cm long thin aluminum tube to create a single mass M, formed by the middle and outer gliders. This pulled gliders #2 and #4 further away from the center glider. Additionally, because gliders #1, #3 and #5 were rigidly attached, the mass of the three gliders combined to give the larger mass, M, and enabled the system to achieve lower mass ratios.

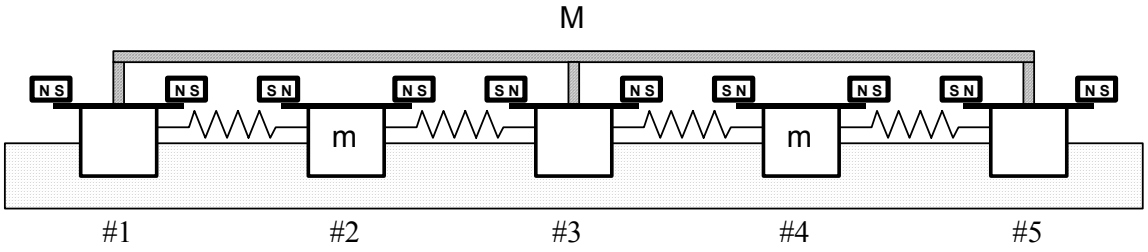


Figure 22. Double-spring air track glider system setup to mimic a triatomic molecule using five spring coupled gliders. Gliders #1, #3, #5 are rigidly coupled to form mass M.

The tube is attached to the gliders by posts with washers, where it is important to note that the washers must be carefully inserted or removed such that the entire M mass moves with little friction. Without such an adjustment, an excessive downward force due to the aluminum tube can cause a glider to stick on the track. In addition, the attached gliders must be free to swivel, so that friction is minimized. We use a Daedalon 2.5 m air track with a gold-colored (0.15 kg) for each m mass and three blue (0.45 kg) gliders connected together for the M mass. We also use Daedalon 2.5 cm springs. (Daedalon) The air track is driven by two air pumps, one attached to each end.

Another particular problem involves symmetry. If a system is not symmetric, then releasing the gliders in the simple manner described above will not lead to pure excitation of a normal mode, so linear beating will occur between the normal modes. This is unacceptable in our case, because the signature of the parametric instability is a nonlinear beating between the modes. Due primarily to variations in the spring constants of the springs, we expended a substantial amount of effort in arranging the system in Fig. 22 to be sufficiently symmetric. Our test for the symmetry was the absence of linear beating for our simple initial conditions.

In the initial investigation the gliders remained connected by two springs, one mounted on each side of all five gliders. Mass ratios between 0.269 and 0.8 were achieved. It was found that neither of the oscillatory normal modes exhibited the instability, even at large amplitudes and small mass ratios.

In the second system each of the gliders were coupled by a single 2.5 cm spring. Figure 23 is a picture of the actual apparatus developed. This was a revised version of the double-spring air track glider system described previously. Holes were drilled in the gliders to attach a single spring 2-mm above the air track and 2-cm below the magnets. The separation distance between gliders was 21.25-cm. At large amplitudes of the motion, the m gliders can depart from the air track. Because the threshold amplitude for the instability decreases as $\rho$ decreases, the value of $\rho$ must be sufficiently small such that the instability occurs before the gliders depart from the air track, but not so small that the linear motion below the amplitude threshold cannot be clearly demonstrated. To achieve this, as stated earlier, we use blue gliders for the M mass and gold gliders for the m masses. In addition, we add a 100-gram mass to each of the two sides of each outer glider. The resultant mass ratio (which includes the aluminum tube, posts, and magnets) is $\rho = 0.11$. The lower-frequency mode is observed to be stable at all amplitudes, where as the upper-frequency mode is observed to be stable at smaller amplitudes and unstable at larger amplitudes.

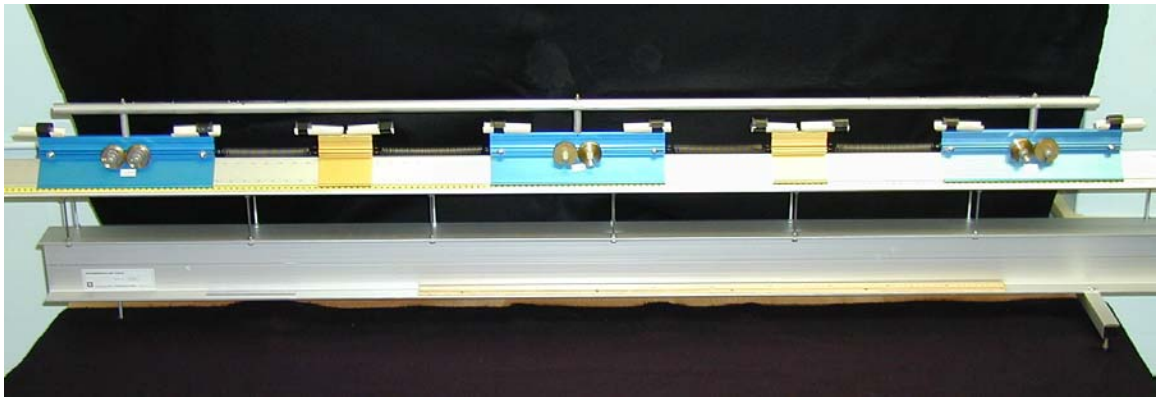

Figure 23. Picture of actual air track glider system utilizing repulsive magnets and coupled with single springs to demonstrate the instability in the upper-frequency hardening mode, $\rho = 0.11$.

First, gliders #2 & #4 were displaced 2.0-cm in the same direction followed by 2-cm in the opposite direction to ensure the upper and lower frequency modes were stable at low amplitudes and the system is symmetric. Then, gliders #2 and #4 were displaced 7.0 cm in opposite directions to see if there was any instability in the lower frequency mode, there was none. This displacement distance was chosen because it was the maximum displacement which did not cause chaotic behavior in the gliders, resulting in rubbing between the glider and the air track or resulting in gliders #2 & #4 jumping off the air track. Thorough examination demonstrated that this mode of vibration was stable even when the gliders were not displaced exactly equal. Instead of this mode becoming unstable, the entire system would also exhibit the zero-frequency mode and translate down the track. Finally, gliders #2 and #4 were displaced in the same direction 7.0 cm to look for the instability. After thorough examination, $\rho = 0.127$ was discovered to be the minimum mass ratio to exhibit the principal parametric instability under the above conditions.

## E. SOFTENING (SLANTED-SPRING) AIR TRACK GLIDER SYSTEM

Figure 24 shows the top view of a softening system, for which the lower-frequency mode should be unstable above an amplitude threshold. To leading nonlinear order, a calculation shows that the slanted springs give rise to a softening cubic nonlinearity in the force, as long as the springs are sufficiently nonperpendicular to the track (App. C). Specifically, the distance from the center of an m glider to the attachment point of the spring on the transverse rod must be less than half the distance between the centers of an m glider and the central M glider in equilibrium. In our apparatus, the springs were initially at roughly 45°. We did not observe the predicted instability, even for the maximum amplitude in which the gliders touch.

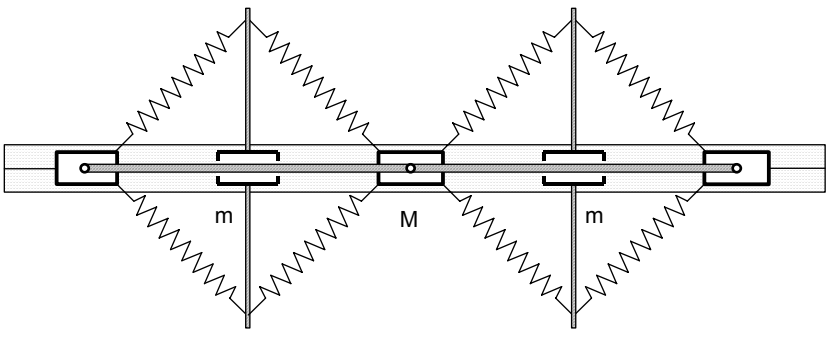


Figure 24. Top view of the slanted-spring air track glider system

Calculation showed that in order to maximize the softening force in the system the length, b, from the center of glider m to the attachment point of the spring on the transverse rail had to be approximately 0.7a, where a here is the distance from the end of glider M to the center of glider m and the length of the unstreached spring, c, had to be approximately 1.2a, see Fig. 25. In this figure, the ordinate is the ratio of the nonlinear coefficient to the linear coefficient in the force. (Refer to App. C.) Unfortunately, the optimized system was not achievable due to a large variability in the Daedelon springs, which prevented symmetrization. This was true even though the springs had the same length and radius, were made with the same diameter of wire, and came from the same lot number. Pairs of 2.5 and 7.5 cm springs were used for the system in Fig. 24.

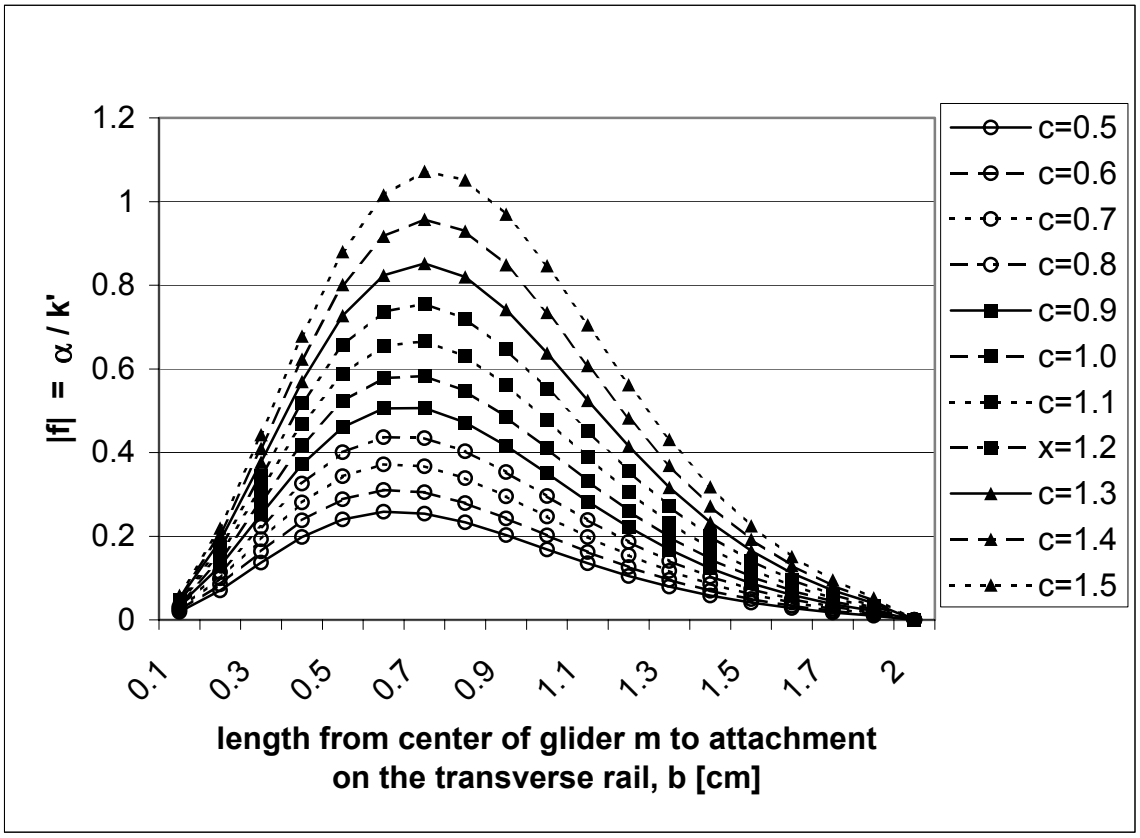


Figure 25. Calculation of maximum softening force for varying lengths in the slanted-spring air glider demonstration.

The lowest value of b obtained for this system while maintaining symmetry in the springs was b = 16 cm. The threshold amplitude required to initiate the instability in this system was calculated from Eq. (11), where $\omega_0^2 = 2\pi f_0$, $\rho = m/M$, and $\alpha = (2k/m)(4a^2-b^2)/(a^2+b^2)^{7/2}b^2c$, a = 23 cm, b = 16 cm, c = 16.8 cm, m = 178.5 g, M = 2624 g. The

spring constants were computed to be k = 951 dynes/cm. From this the threshold amplitude was determined to be 14.5 cm and the maximum amplitude achievable in the system was 18.5 cm. It was apparent that the system was above threshold, however, after two oscillations the amplitude decreased below the threshold amplitude. This may not be enough time for the instability to develop.

To increase the softening nonlinearity and assist the system in remaining above the threshold amplitude for inducing the instability, attractive magnets were added to the system (Fig. 26). The same magnet assembly used in Sec. IV.E, was used in the slanted-spring assembly. However, to keep the maximum amplitude of the system at the same value as in Sec. IV.F the magnets on gliders #1, #3, and #5 were recessed toward the center of each glider 8.5 cm. Because the threshold amplitude for the instability decreases as $\rho$ decreases, the value of $\rho$ must be sufficiently small such that the instability occurs before the gliders hit, but not so small that the linear motion below the amplitude threshold cannot be clearly demonstrated. To achieve this, we use blue gliders for the M masses and gold gliders for the m masses. In addition, I added 150 grams of mass to each of the two sides of each outer glider and 200 grams of mass to each of the two sides of the middle glider. The resultant mass ratio (which includes the aluminum tube, posts, and magnets) is $\rho = 0.095$. The lower-frequency mode is observed to be stable at all amplitudes, wheras the upper-frequency mode is observed to be stable at smaller amplitudes and unstable at larger amplitudes.

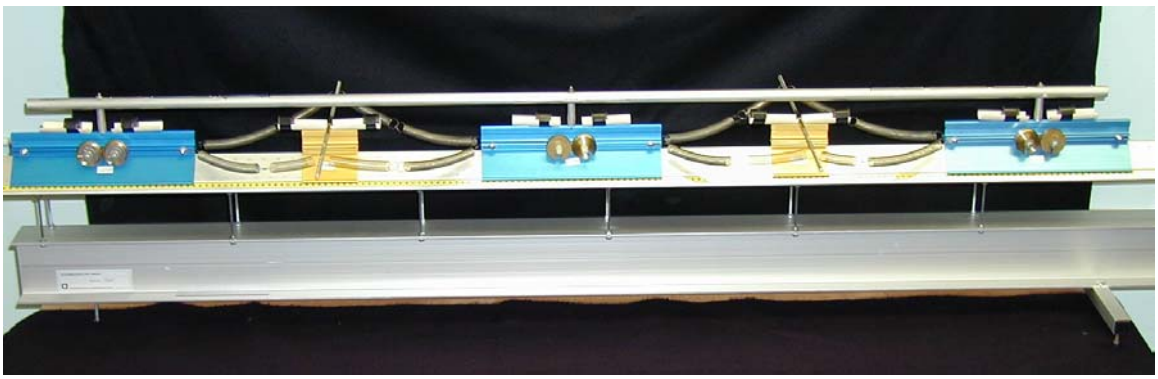

Figure 26. Picture of actual air track glider system utilizing attractive magnets and coupled with two slanted springs to demonstrate the instability in the lower-frequency hardening mode, $\rho = 0.095$.

First, gliders #2 & #4 were displaced 2.0 cm in the same direction followed by 2 cm in the opposite direction to ensure the upper and lower frequency modes were stable at low amplitudes and the system is symmetric. Then, gliders #2 and #4 were displaced 18.0 cm in the same direction to confirm that there was no instability in the upper-frequency mode. This displacement distance was chosen because it was the maximum displacement that did not cause collisions between gliders, resulting in decreased amplitudes between gliders and induced beating. Thorough examination demonstrated that this mode of vibration was stable even when the gliders were not displaced exactly equal. Instead of this mode becoming unstable, the entire system would also exhibit the zero frequency mode and translate down the track. Finally, gliders #2 and #4 were displaced in opposite directions 18.0 cm to look for the instability. The principal parametric instability appeared evident but was very weak. To increase the instability on the system, the mass ratio was reduced to $\rho = 0.089$ by adding an additional 200 grams of mass to each of the two sides of the end and middle gliders. Contrary to the initial assumption, the instability decreased. The reason for this behavior is that decreasing $\rho$ decreases the threshold amplitude, but longer time is required for the instability to develop.

# V. CONCLUSIONS

Due to nonlinearity, a normal oscillatory mode of a system can parametrically drive another normal oscillatory mode. Through conservation of energy, the initially excited mode of a nonlinearly coupled system must be unstable. We have investigated a parametric instability of a simple model of a classical triatomic molecule. The system is rectilinear and symmetric, and the coupling includes a cubic nonlinearity in the force. The instability is expected to occur for the classical motion of a wide variety of molecules with more than one oscillatory mode.

Our results are important for two reasons. First, the classical linear motion of a rectilinear symmetric molecule is commonly taught in physics as an interesting example of linear normal mode theory. The energy of each normal mode remains constant in this case. We have shown that nonlinearity can dramatically alter this. Second, the existence of the instability raises interesting questions about the oscillatory behavior of actual (quantum mechanical) molecules. As example, the specific heat of a gas of the molecules may be lowered. As another example, the transition probability to higher energy levels may be enhanced, which could be exploited in the operation of some lasers.

The instability occurs for amplitudes above a threshold value, where this value decreases as the difference in frequency of the two normal modes is reduced. For a softening nonlinearity, the lower-frequency normal mode can be unstable, while for a hardening nonlinearity, the upper-frequency normal mode can be unstable. Numerical simulations agree well with the analytical predictions, although some interesting deviations were observed. For example, parametric resonances other than the principal resonance can occur when the ratio of the outer masses to the central mass is not small. In addition, if the mass ratio is very small, the principal resonance was observed to occur when the theory predicts it does not occur. This is interesting because it represents behavior that is fundamentally different than that which the standard leading-order perturbation theory predicts.

I constructed an apparatus that demonstrates the instability in the case of both the hardening upper-frequency mode and softening lower-frequency mode. The hardening

system consists of gliders on an air track, where springs and repulsive magnets supply the coupling. In accord with the theory, the upper-frequency mode is observed to be unstable for amplitudes above a threshold value. The resultant motion is a beating between the two normal modes. Also in accord with theory, the lower-frequency mode is observed to be stable at all amplitudes. Difficulty in observing the nonlinearity in the hardening system may be attributed to the strong linear restoring force in the double spring coupling utilized in the first demonstration. Additionally, there is some linearity associated with the magnets. Only when the linearity was reduced to a minimum, the nonlinearity was increased to a maximum and the large mass was increased to a maximum for this system was the instability evident. The aforementioned conditions were met by reducing the system to a single spring, extending the magnets as far as the apparatus would allow, and weighing down the apparatus as much as the system could handle without introducing friction.

The softening system consists of gliders on an air track, where slanted-springs and attractive magnets supply the coupling. Both the slanted-springs and the attractive magnets provide a softening restoring force to the system. In accord with the theory, the lower-frequency mode is observed to be unstable for amplitudes above a threshold value. The resultant motion is a beating between the two normal modes. Also in accord with theory, the upper-frequency mode is observed to be stable at all amplitudes. Difficulty in seeing the nonlinearity in the softening system may be attributed to the apparent weakness of the nonlinearity in the arrangement and a quick decay of the initial amplitude of the motion supplied to the system. Even after the first slanted-spring system was optimized to supply the largest softening force possible, the system never oscillated more than twice above the amplitude threshold for the system. Introducing the attractive magnets into the system helped extend the lifetime of oscillations above the threshold amplitude so that the system could exhibit the instability.

# VI. FUTURE WORK

According to our extensive literature search, an instability of a mode due to the mode parametrically driving another mode has not been investigated for quantum mechanical systems. A possible interesting consequence of this is that a gas of triatomic molecules that classically exhibit such an instability may have a specific heat that is less than the predicted value. This should be analytically investigated and experiments could be performed.

Another interesting quantum mechanical possibility that should be investigated is that the transition probability due to absorption of radiation or collisions could be enhanced in cases where the instability cannot proceed because it would violate energy conservation. This could have a beneficial consequence for some lasers.

Our numerical simulations for a softening nonlinearity were subject to the "over-the-top" instability, which occurred before the parametric instability may have ceased to occur. This possible upper threshold is interesting because it would be beyond the standard perturbation theory. The effect can be numerically probed by using a softening potential energy that does not negatively diverge. An example of such a potential energy is $\ln(1 + x^2)$ (in dimensionless units).

Our numerical simulations revealed that parametric resonances other than the principal resonance readily occur. These cases can be analytically investigated and the results can be compared to the numerical simulation data.

Our successful demonstrations were only partially quantitative; we did not fully quantify them in order to compare the results to the theory. The demonstrations could become quantitative experiments if the force vs. displacement is statically measured, which would allow the nonlinear coefficient to be determined. Alternatively, the nonlinear coefficient could be determined from amplitude-dependent period measurements. The nonlinear coefficient due to the magnets could be quantified to ensure that the demonstrations exhibited the instability due to the principal parametric resonance and not due to nonuniformity of the magnets.

I did not create a demonstration of the instability for a triatomic molecule with softening nonlinearity, using only slanted-springs with gliders on an air track. This arrangement appears to be inherently only weakly nonlinear, so that the threshold amplitude for the instability is difficult to obtain for an actual system. More work needs to be done with the slanted-spring arrangement to ascertain whether it can be used to convincingly demonstrate the instability. A complicating factor is that the system must be symmetric so that simple sets of initial conditions correspond to the normal modes of the system. Otherwise, linear beating will occur, which would mask the nonlinear beating due to the instability.

Finally, actual molecules do not have symmetric potentials. That is, they are approximately modeled by both cubic and quadratic nonlinear terms in the force. The theory for this should be done, and should be a straightforward generalization of our theory with just a cubic nonlinearity. The theory may explain why our preliminary asymmetric potential arrangement with air track gliders, springs, and magnets failed to exhibit the instability. It should be noted that an alternative demonstration with cubic and quadratic nonlinearities can be obtained if the outer or inner pairs of magnets are removed in our successful cubically nonlinear glider system. It should also be noted that this demonstration could become a quantitative experiment.

# APPENDIX A: NUMERICAL SIMULATION PROGRAMS

## A. LOWER-FREQUENCY MODE PROGRAM

```
/*****************************************************************

                              lower.cpp

This program determines whether the lower-frequency (antisymmetric) mode of a
triatomic molecule is stable or unstable for a specified amplitude.  The equations
of motion are
x" + x = alpha*(x^3 + 3*gamma^2*x*y^2)

y" + gamma*y = alpha*(gamma^3*y^3 + 3*gamma*x^2*y) ,

where x is the lower-frequency (antisymmetric) mode and y is the upper-
frequency (symmetric) mode.

*****************************************************************/

#include <stdio.h>
#include <stdlib.h>
#include <math.h>

#define     dt          0.0001

#define     epsilon     0.0001

#define     criterion   0.001

#define     tmax        100

#define     alpha       -1.0

void main()
{
        double A, rho, gamma, gamma2, gamma3, over;
        double t, x, y, u, v;
        double unonlin, vnonlin;
        double xsq, ysq, xnew, ynew, unew, vnew;
        int answer, flag;

MASSRATIO:

        printf("Enter mass ratio m/M:  ");
        scanf("%lf", &rho);
```

```
        printf("\n");
        gamma = 1.0 + 2.0*rho;
        gamma2 = gamma*gamma;
        gamma3 = gamma*gamma2;

        over = 1.0 + criterion;

AMPLITUDE:

        printf("Enter amplitude of lower mode:  ");
        scanf("%lf", &A);
        printf("\n");

        FILE *fout;
        fout = fopen("dataout.dat", "w");

        x = A;
        u = 0.0;

        y = epsilon;
        v = 0.0;

        flag = 0;

        for (t = 0.0; t <= tmax; t = t + dt)
        {
                xsq = x*x;
                ysq = y*y;

                unonlin = alpha*(x*xsq + 3.0*gamma2*x*ysq);
                vnonlin = alpha*(gamma3*y*ysq + 3.0*gamma*xsq*y);

                unew = u + (-x + unonlin)*dt;
                vnew = v + (-gamma*y + vnonlin)*dt;
                xnew = x + unew*dt;
                ynew = y + vnew*dt;

                fprintf(fout,"%f \t %f \t %f \n", t, x, y);

                if (y > criterion) flag = 1;
                if (alpha > 0.0 && fabs(x) > over) goto OVERTOP;

                x = xnew;
                y = ynew;
                u = unew;
                v = vnew;
```

```
        }

        fclose(fout);

        if (flag == 1) goto UNSTABLE;

QUESTION:

        printf("STABLE.  New amplitude (1), new mass ratio (2), or end (0)?  ");
        scanf("%i", &answer);
        printf("\n");

        if (answer == 0) goto END;
        if (answer == 1) goto AMPLITUDE;
        if (answer == 2) goto MASSRATIO;
        goto QUESTION;

UNSTABLE:

        printf("UNSTABLE:  Growth of upper mode. \n");
        goto QUESTION2;

OVERTOP:

        printf("UNSTABLE:  Over-the-top motion. \n");

QUESTION2:

        printf("New amplitude (1), new mass ratio (2), or end (0)?  ");
        scanf("%i", &answer);
        printf("\n");

        if (answer == 0) goto END;
        if (answer == 1) goto AMPLITUDE;
        if (answer == 2) goto MASSRATIO;
        goto QUESTION2;

END:

        printf("End of program.\n\n");
}
```

## B. UPPER-FREQUENCY MODE PROGRAM

```
/*****************************************************************

                                upper.cpp

This program determines whether the upper-frequency (symmetric)
mode of a triatomic molecule is stable or unstable for a specified
amplitude.  The equations of motion are

        x" + x = alpha*(x^3 + 3*gamma^2*x*y^2)

        y" + gamma*y = alpha*(gamma^3*y^3 + 3*gamma*x^2*y) ,

where x is the lower-frequency (antisymmetric) mode and y is the
upper-frequency (symmetric) mode.


*****************************************************************/

#include <stdio.h>
#include <stdlib.h>
#include <math.h>

#define         dt              0.001

#define         epsilon         0.0001

#define         criterion       0.01

#define         tmax            1000

#define         alpha           -1.0

void main()
{
        double A, rho, gamma, gamma2, gamma3, over;
        double t, x, y, u, v;
        double unonlin, vnonlin;
        double xsq, ysq, xnew, ynew, unew, vnew;
        int answer, flag;

MASSRATIO:

        printf("Enter mass ratio m/M:  ");
        scanf("%lf", &rho);
        printf("\n");
```

```
        gamma = 1.0 + 2.0*rho;
        gamma2 = gamma*gamma;
        gamma3 = gamma*gamma2;

        over = 1.0/gamma + criterion;

AMPLITUDE:

        printf("Enter amplitude of upper mode:  ");
        scanf("%lf", &A);
        printf("\n");

        FILE *fout;
        fout = fopen("dataout.dat", "w");

        x = epsilon;
        u = 0.0;

        y = A;
        v = 0.0;

        flag = 0;

        for (t = 0.0; t <= tmax; t = t + dt)
        {
                xsq = x*x;
                ysq = y*y;

                unonlin = alpha*(x*xsq + 3.0*gamma2*x*ysq);
                vnonlin = alpha*(gamma3*y*ysq + 3.0*gamma*xsq*y);

                unew = u + (-x + unonlin)*dt;
                vnew = v + (-gamma*y + vnonlin)*dt;
                xnew = x + unew*dt;
                ynew = y + vnew*dt;
/*
                fprintf(fout,"%f \t %f \t %f \n", t, x, y);
*/
                if (x > criterion) flag = 1;
                if (alpha > 0.0 && fabs(y) > over) goto OVERTOP;

                x = xnew;
                y = ynew;
                u = unew;
                v = vnew;
        }
```

```
        fclose(fout);

        if (flag == 1) goto UNSTABLE;

QUESTION:

        printf("STABLE.  New amplitude (1), new mass ratio (2), or end (0)?  ");
        scanf("%i", &answer);
        printf("\n");

        if (answer == 0) goto END;
        if (answer == 1) goto AMPLITUDE;
        if (answer == 2) goto MASSRATIO;
        goto QUESTION;

UNSTABLE:

        printf("UNSTABLE:  Growth of lower mode. \n");
        goto QUESTION2;

OVERTOP:

        printf("UNSTABLE:  Over-the-top motion. \n");

QUESTION2:

        printf("New amplitude (1), new mass ratio (2), or end (0)?  ");
        scanf("%i", &answer);
        printf("\n");

        if (answer == 0) goto END;
        if (answer == 1) goto AMPLITUDE;
        if (answer == 2) goto MASSRATIO;
        goto QUESTION2;

END:

        printf("End of program.\n\n");
}
```

# APPENDIX B: HIGHER ORDER PARAMETRIC RESONANCES IN LOWER FREQUENCY MODE WITH HARDENING NONLINEARITY

The following graphs demonstrate the different parametric resonances and can be understood by examining the ratio, $f_r/f_d$, of the response frequency to the drive frequency. For the principal, isochronous, third order, and fourth order parametric resonances, $f_r/f_d$ = ½, 1, 3/2, 2, respectively. Due to the nonlinearity, the mode being parametrically excited experiences a drive at twice the frequency of the initial mode.

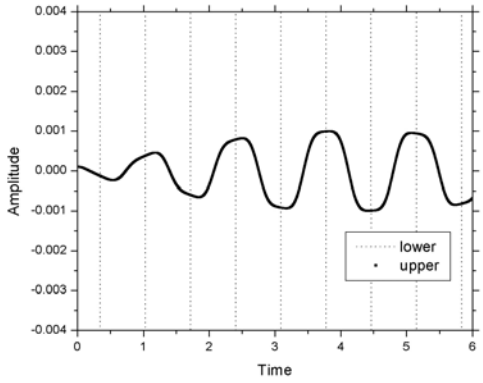


Figure B.1. Example of principal parametric resonance in the lower-frequency hardening mode, ρ = 0.009, A =5.26300, δt = 0.001, epsilon = 0.0001, criterion 0.001.

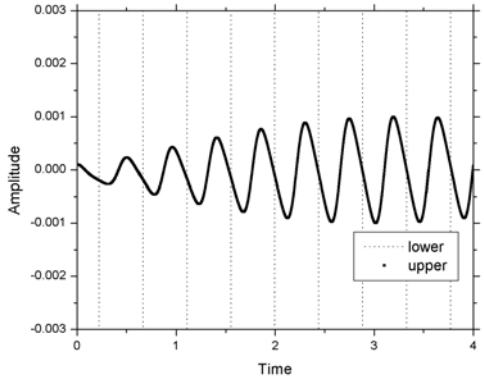


Figure B.2. Example of isochronous parametric resonance in the lower-frequency hardening mode, ρ = 0.5, A =8.2693, δt = 0.001, epsilon = 0.0001, criterion 0.001.

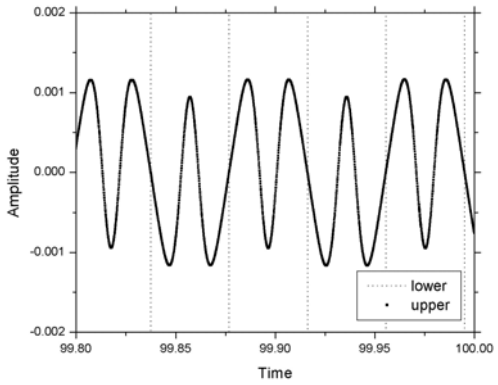


Figure B.3. Example of third order parametric resonance in the lower-frequency hardening mode, r = 2.0, A = 94.09, δt = 0.0001, epsilon = 0.0001, criterion 0.001.

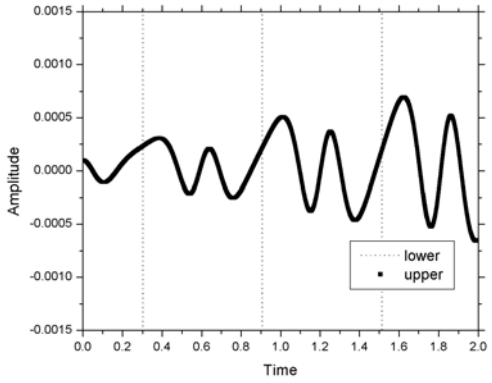


Figure B.4. Example of fourth order parametric resonance in the lower-frequency hardening mode, r = 4.2, A = 6.006, δt = 0.0001, epsilon = 0.0001, criterion 0.001.

# APPENDIX C: NONLINEAR BEHAVIOR OF A SLANTED-SPRING OSCILLATOR

A demonstration of a classical triatomic molecule in which the coupling *hardens* (slope of force vs. displacement increases with amplitude) can readily be obtained with springs and magnets (Sec. IV.D). We also desire a demonstration in which the coupling *softens* (slope of force vs. displacement curve decreases). Although it is not obvious, such a situation can be obtained with a slanted-spring arrangement (Fig. C.1). In this section, we determine the leading (cubic) order nonlinearity in terms of the parameters of the system, and thereby determine the conditions for which the slanted spring oscillator softens.

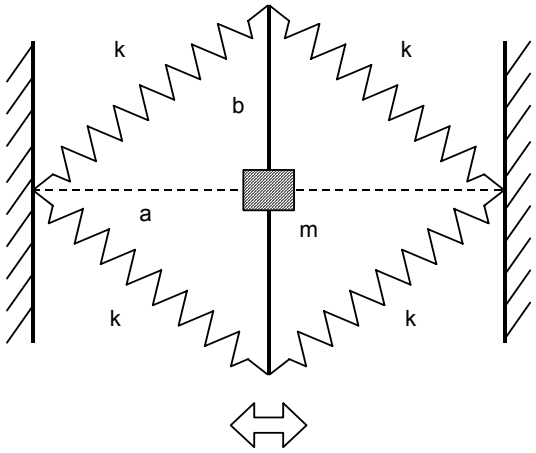


Figure C.1. Slanted-spring oscillator in equilibrium. The mass oscillates back and forth as denoted by the arrow. This is a *nonlinear* oscillator; Hooke's law only holds approximately for small amplitudes.

We let the unstretched length of each spring be c. For any displacement x, we can determine the force from Fig. C.2. For practical purposes, it is assumed that $|x| < a$ and c is sufficiently small such that each spring never compresses. However, the theory holds for any displacement and for any values of the parameters. The net force on the mass m is

$$\begin{aligned} F = &-2k\left[\sqrt{(a+x)^2+b^2}-c\right]\cos(\theta) \\ &+\ 2k\left[\sqrt{(a-x)^2+b^2}-c\right]\cos(\varphi) \end{aligned} \tag{C.1}$$

Substituting the relationships

$$\cos(\theta) = \frac{a+x}{\sqrt{(a+x)^2 + b^2}} \quad \text{and} \quad \cos(\varphi) = \frac{a-x}{\sqrt{(a-x)^2 + b^2}} ,$$

and simplifying, we find that

$$\begin{aligned} F = &-2k\left[1 - \frac{c}{\sqrt{(a+x)^2 + b^2}}\right](a+x) \\ &+ 2k\left[1 - \frac{c}{\sqrt{(a-x)^2 + b^2}}\right](a-x) \end{aligned} \tag{C.2}$$

This gives the exact force as a function of the displacement.

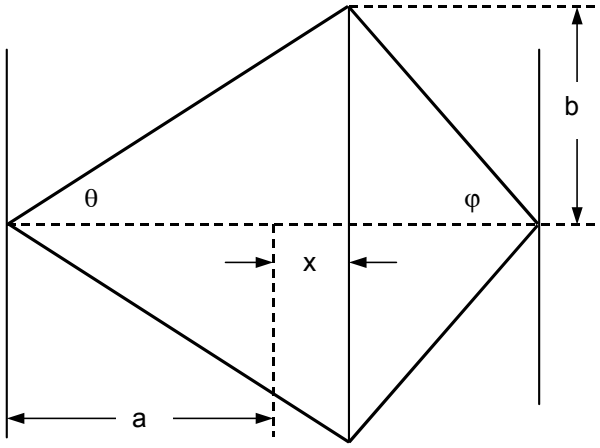


Figure C.2. Essential geometry of a slanted-spring oscillator displaced a distance x from equilibrium.

Before expanding Eq. (C.2) in a Taylor expansion in x, we consider a graph of |F| vs. x for k = 1/4 and a = b = c = 1. The result is shown in Fig. C.3, which reveals that the force softens. This is surprising. As the displacement increases, the restoring springs become more longitudinal and the anti-restoring springs to become more perpendicular, which causes the slope of force vs. displacement to increase. That is, in Eq. (C.1) the cos(θ) factor increases and the cos(φ) factor decreases. Hence, it is expected that the

system hardens. However, in addition to this effect, the length of each spring softens with increasing x. This second effect evidently dominates the first.

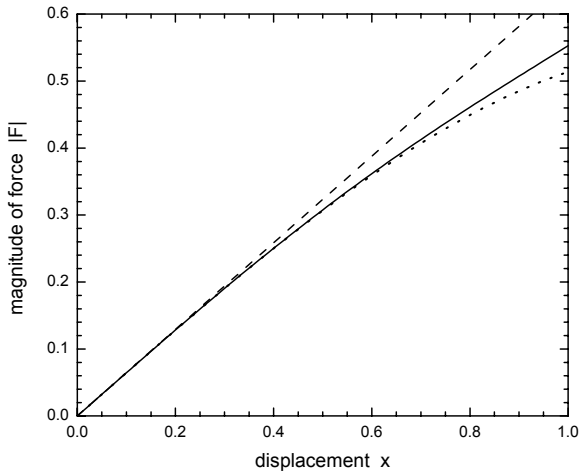


Fig. C.3. Exact (nonperturbative) magnitude of the force vs. displacement for a slanted-spring oscillator. The parameters are k = 1/4 and a = b = c = 1, where c is the unstretched length of each spring. The dashed line, which has slope $1 - 2^{-3/2}$, is Hooke's law in the limit of small displacements. The dotted curve is the result of the perturbative theory, which is valid to third order in the displacement.

For small displacements, we can expand Eq. (C.2) to third order in x. This requires a substantial amount of algebra. We begin by noting that

$$\sqrt{(a+x)^2+b^2} = \sqrt{a^2+b^2}\sqrt{1+\frac{2ax+x^2}{a^2+b^2}} \ . \qquad \text{(C.3)}$$

The quantity $[(a - x)^2 + b^2]^{1/2}$ can be obtained by simply replacing x with –x in this expression. Next, we use the expansion

$$\frac{1}{\sqrt{1+\varepsilon}} = 1-\frac{1}{2}\varepsilon+\frac{3}{8}\varepsilon^2-\frac{5}{16}\varepsilon^3+\cdots \ .$$

Substituting $\varepsilon = (2ax + x^2)/(a^2 + b^2)$, retaining terms only to cubic order in x, grouping terms according to the power of x, and simplifying, yields the following from Eq. (C.3):

$$\frac{\sqrt{a^2+b^2}}{\sqrt{(a+x)^2+b^2}} = 1 - \frac{a}{a^2+b^2}x + \frac{2a^2-b^2}{2\left(a^2+b^2\right)^2}x^2 - \frac{2a^3-3ab^2}{2\left(a^2+b^2\right)^3}x^3 \ .$$

In view of Eq. (C.2), we multiply this by a + x, expand to third order in x, and simplify. The result is

$$\frac{\sqrt{a^2+b^2}}{\sqrt{(a+x)^2+b^2}}(a+x) = a + \frac{b^2}{a^2+b^2}x - \frac{3ab^2}{2\left(a^2+b^2\right)^2}x^2 + \frac{4a^2b^2-b^4}{2\left(a^2+b^2\right)^3}x^3 \ .$$

Finally, we substitute this expression into Eq. (C.2) to determine the force. Due to the symmetry, all even terms in x cancel, and the result is

$$F = -4k\left[1 - \frac{b^2c}{\left(a^2+b^2\right)^{3/2}}\right]x + 2k\frac{4a^2-b^2}{\left(a^2+b^2\right)^{7/2}}b^2cx^3 \ . \qquad \text{(C.4)}$$

There are several special cases of the result (C.4) that can be considered. First, note that if b = 0 (longitudinal oscillator), then the equation yields the correct result F = –4kx, independent of c. Second, if a = 0 (transverse oscillator), then Eq. (C.4) reveals that the oscillator is always hardening if $c \neq 0$. Third, if c = 0, then Eq. (C.4) yields F = –4kx, independent of a and b. This is perhaps a surprising result, although from Eq. (C.2) it is immediately seen to be valid exactly (to all orders of x).

As shown in Fig. C.3, for the parameters k = 1/4 and a = b = c = 1, the result (C.4) agrees very well with the exact force if the displacement is small. The deviation is a maximum at the maximum displacement of unity, as expected, and this deviation is 7.5%. The result (C.4) shows that the slanted-spring oscillator softens if 2a > b, provided $b \neq 0$ and $c \neq 0$. We confirmed this approximate result by plotting the exact force (C.2) for k = 1/4 and a = c = 1, with b = 1.8 and 2.2. The curves are nearly straight lines, with the b = 1.8 curve having negative curvature and the b = 2.2 curve having positive curvature.

# LIST OF REFERENCES

(Beiser)Arthur Beiser, Concepts of Modern Physics, 5th ed. (McGraw-Hill, New York, 1995), pp 284-291.

(Daedalon)Daedalon Corp. (Salem, Massachusetts, 800-233-2490, daedalon@cove.com). Product numbers: air track EA-76, gliders EA-05, EA-06, EA-07, and springs EA-33.

(Denardo)Bruce Denardo, John Earwood, and Vera Sazonova, "Parametric instability of two coupled nonlinear oscillators," Am. J. Phys. v..**67**, pp.187-195 (1999).

(Fowles)Grant R. Fowles and George L. Cassiday, *Analytical Mechanics*, 6th ed. (Saunders, Fort Worth, 1999), pp. 466-468.

(Garcia)Alejandro L. Garcia, *Numerical Methods for Physics,* 2nd ed. (Prentice Hall, Upper Saddle River, New Jersey, 2000), p. 41.

(Goldstein)Herbert Goldstein, *Classical Mechanics*, 2nd ed. (Addison-Wesley, Reading, 1980), pp. 258-263.

(Landau)L. D. Landau and E. M. Lifshitz, *Mechanics*, 3rd ed. (Pergamon, New York, 1976), p. 72.

(Marion)Jerry B. Marion and Stephen T. Thornton, *Classical Dynamics of Particles and Systems*, 4th ed. (Saunders, Fort Worth, 1995), pp. 482-486.

(Quantum)For example, see the following: M. S. Marinov and E. Strahov, "A geometric approach to non-adiabatic transitions in quantum theory: Applications to NMR, over-barrier reflection, and parametric excitation of a quantum oscillator," J. Phys. A: Math. Gen. **34**, 1741-1752 (2001); P. G. Kevrekidis, A. R. Bishop, and K. O. Rasmussen, "Parametric quantum resonances for Bose-Einstein condensates," J. Low Temp. Phys. **120**, 205-212 (2000); S. N. Bagaev, V. S. Egorov, P. V. Moroshkin, A. N. Fedorov, and I. A. Chekhonin, "Gain and lasing in two-level optically dense resonance media without population inversion based on cooperative phenomena upon interaction of light with matter," Opt. and Spect. **86**, 814-819 (1999); Christine Zerbe and Peter Hänggi, "Brownian parametric quantum oscillator with dissipation," Phys. Rev. E **52**, 1533-1543 (1995); S. T. Dembiński, A. J. Makowski, and P. Peplowski, "Quantum bouncer with chaos," Phys. Rev. Lett. **70**, 1093-1096 (1993); Petr Seba, "Quantum chaos in the Fermi-accelerator model," Phys. Rev. A **41**, 2306-2310 (1990).

THIS PAGE INTENTIONALLY LEFT BLANK

# INITIAL DISTRIBUTION LIST

1. Defense Technical Information Center
   Ft. Belvoir, Virginia

2. Dudley Knox Library
   Naval Postgraduate School
   Monterey, California

3. Physics Department
   Naval Postgraduate School

   Monterey, CA 93943-5002

4. Professor Bruce Denardo, Code PH/De
   Department of Physics
   Naval Postgraduate School
   Monterey, CA 93943-5002

5. Professor Andres Larraza, Code PH/La
   Department of Physics
   Naval Postgraduate School
   Monterey, CA 93943-5002

6. Professor James Luscombe, Code PH/Lj
   Department of Physics
   Naval Postgraduate School
   Monterey, CA 93943-5002

7. Combat Systems Curricular Office, Code 34
   Naval Postgraduate School
   Monterey, CA 93943-5101